JOURNAL OF PETROLOGY | VOLUME 49 | NUMBER 11 | PAGES 1931–1953 | 2008 | doi:10.1093/petrology/egn052

Concurrent Mixing and Cooling of Melts under Iceland

J. MACLENNAN*

DEPARTMENT OF EARTH SCIENCES, UNIVERSITY OF CAMBRIDGE, CAMBRIDGE CB2 3EQ, UK

RECEIVED NOVEMBER 7, 2007; ACCEPTED SEPTEMBER 25, 2008
ADVANCE ACCESS PUBLICATION OCTOBER 29, 2008

The compositions of 75 melt inclusions, their host olivines and 49 whole-rock samples of their carrier lavas have been determined. These compositions were added to a compilation of the trace element composition of 243 melt inclusions from 10 eruptions in the neovolcanic zones of Iceland and used to investigate melt mixing processes. Whereas the compositional variability of whole-rock samples from single eruptions is limited, there are significant compositional differences between eruptions. The compositions of inclusions are more variable than those of whole-rock samples of their carrier lava. On a flow-by-flow basis, the average composition of trace element ratios such as La/Yb in the inclusions is similar to that of their carrier lava. These observations indicate that, for each lava flow, melts with compositions similar to those of the inclusions crystallized and mixed to produce the magma that transported the host olivines to the surface. Although many of the olivines are not in Mg–Fe equilibrium with their host melt, they are not accidental xenocrysts because they crystallized from melts similar to those that mixed to form the carrier magma. The trace element variability of melt inclusions drops with decreasing forsterite content of the host olivine. This relationship is observed both within single flows and in the compilation of data from 10 flows. Concurrent mixing and crystallization dominate the compositional evolution of basaltic melts in lower crustal magma chambers. This coupled mixing and cooling is likely to result from convective motions in magma chambers. The rate of change of the mixing parameter, M, *with temperature of the melt is* $\mathrm{d}M/\mathrm{d}T = 0{\cdot}0094 \pm 0{\cdot}0036$ *per* °*C. This relative rate may be used to constrain the fluid dynamics of basaltic magma chambers.*

KEY WORDS: *basalt; crystallization; Iceland; magma chamber; mixing*

INTRODUCTION

Generation of melt in the mantle is thought to be dominated by fractional melting (Kelemen *et al.*, 1997). Models of fractional melting predict that a wide range of melt compositions are produced during melting. The observed range of compositions of basalts from mid-ocean ridges and ocean islands is much less than that predicted for instantaneous fractional melts from melting models. Furthermore, the trace element and isotopic compositions of melt inclusions are known to be far more variable than those of their carrier magmas (Sobolev & Shimizu, 1993; Saal *et al.*, 1998). These observations demonstrate the importance of melt mixing in controlling the composition of magma. However, the melt mixing process is not well understood. Some mixing of mantle melts is likely to take place in crustal magma chambers (Sobolev, 1996; Maclennan *et al.*, 2003*a*) but the relative importance of mixing in different environments and its relationship to other processes such as melt transport and crystallization is not yet clear.

The presence of olivine-hosted melt inclusions in the products of many basaltic eruptions provides an opportunity to understand the mixing processes in the roots of these volcanoes. Melt inclusions are trapped in rapidly growing crystals and may therefore record evolution in the compositional heterogeneity of melts in the magmatic system. The composition of olivines growing from basalt is sensitive to the Mg/Fe of the melt, which is, in turn, controlled by cooling and previous crystallization of that melt. Therefore, study of the trace element composition of melt inclusions and the major element composition of their olivine hosts may be used to investigate the relationship between mixing and crystallization. Quantification of the relative rates of mixing and cooling can provide new constraints on fluid dynamical models of magma bodies (Oldenburg *et al.*, 1989; Jellinek & Kerr, 1999).

Trace element variation in melt inclusions may reflect not only compositional heterogeneity of mantle melts but

*Corresponding author. Telephone: +44-1223-761602. Fax: +44-1223-333450. E-mail: jmac05@esc.cam.ac.uk

also shallower processes such as assimilation of crustal melts or localized reaction with cumulate rocks (Danyushevsky *et al.*, 2004; Yaxley *et al.*, 2004; Spandler *et al.*, 2007). To carry out a study of mixing of mantle melts, it is therefore desirable to focus on locations where compositional heterogeneity of melt supply from the mantle has been demonstrated. Isotopic and trace element data from whole-rock samples indicate that the composition of mantle melts generated under the neovolcanic zones of Iceland is variable (Hémond *et al.*, 1993; Stracke *et al.*, 2003; Thirlwall *et al.*, 2004). A recent study of the Reykjanes Peninsula of SW Iceland has shown that olivine-hosted melt inclusions exhibit trace element and isotopic variations coincident with those of whole-rock samples from the region (Maclennan, 2008). Another advantage of studying the neovolcanic zones of Iceland is that plentiful geochemical data are available from eruptions whose locations, volumes and ages are well known. These geological observations provide important constraints upon the significance of melt inclusion compositions and allow investigation of the relationship between melt inclusions, the olivines that host them, and the eruptions that carry these olivines to the surface.

This study is based upon compositional data from a large number of olivine-hosted melt inclusions from the neovolcanic zones of Iceland. These data are used in combination with host olivine and whole-rock compositions to understand the relationship between the inclusion compositions and that of their carrier flow. Then, the evolution of compositional variability in melt inclusions as a function of their host olivine composition is used to provide quantitative constraints on the relative rates of mixing and cooling in magma bodies under Iceland.

TERMINOLOGY

Two points of terminology are worth clarifying to aid understanding of the arguments presented below. The first concerns the description of the processes that occur when two or more batches of melt with distinct compositions are physically juxtaposed. The terminology used in this study is based on the framework of Danckwerts (1953), who sought to quantify the mixing of fluids in chemical engineering. The mixing process takes place in three stages. Initially two melts are physically juxtaposed. Then motions within the fluid body stir the melts together, lengthening the interface between the compositionally distinct domains of fluid and thinning these domains by stretching. When these stretched filaments are sufficiently thin, diffusion may act to homogenize the fluid compositions down to the smallest possible scale. Stirring and diffusion are likely to be concurrent. In the basaltic melts of interest in this paper, we assume that fluid immiscibility is not an important process. Melt or magma mingling may be thought of as equivalent to the juxtaposition phase in the Danckwerts terminology. Complete hybridization of magmas involves not only destruction of compositional variation within the fluid, but also the attainment of chemical equilibrium between phenocrysts in the magma and the mixed carrier melt. The data presented here indicate that whereas melt mixing is often advanced at the time of eruption, magmatic hybridization is incomplete because crystals carried by the melt are variable in composition.

The porphyritic basalts and picrites examined in this study contain large crystals that are straightforward to distinguish from smaller groundmass crystals by visual inspection of crystal shape and size. In this paper, these large crystals are referred to as phenocrysts, in accordance with the etymology of the Greek prefix 'pheno-', meaning to show, appear or display. The advantage of this usage is that genetic associations can be avoided during sample description. The genetic terms xenocryst and antecryst are also defined and used later in the paper, where microanalytical data are used to investigate the relationship between the phenocrysts and the liquid that carries them. In hand specimen, or under an optical microscope, it is seldom possible in practice to distinguish between phenocrysts in equilibrium with their carrier melt, xenocrysts and antecrysts.

SAMPLE COLLECTION AND PREPARATION

Sampling was focused on the Theistareykir and Krafla segments of the Northern Volcanic Zone of Iceland and took place in the summer of 2004. Samples were taken from the recent Krafla eruptions (1975–1984) and the subglacially erupted Gæsafjöll tuya to complement the extensive geochemical dataset available for primitive early postglacial eruptions from this area (Slater *et al.*, 2001; Maclennan *et al.*, 2003*a*, 2003*b*). The locations of these eruptions are shown in Fig. 1, together with the positions of eruptions from which melt-inclusion data are already available. The Krafla samples were taken from lava erupted during the November 1981 and September 1984 rifting episodes. Both basaltic lava samples and tephra were collected and, although they are generally poor in phenocrysts, they contained occasional phenocrysts of olivine, clinopyroxene and plagioclase up to 8 mm in diameter. In contrast, pillow lavas sampled near the base of Gæsafjöll are comparatively rich in olivine (up to 12 vol. %) and plagioclase phenocrysts but contain little clinopyroxene. These pillows were formed near the onset of the eruption as the volcanic edifice built up through a subglacial cavity. Gæsafjöll is capped by subaerial flows, which formed as the eruption penetrated the upper surface of the glacier. Samples were taken both from the pillows with their glassy rims and from the massive interior of subaerial capping flows exposed in tumuli. Samples for

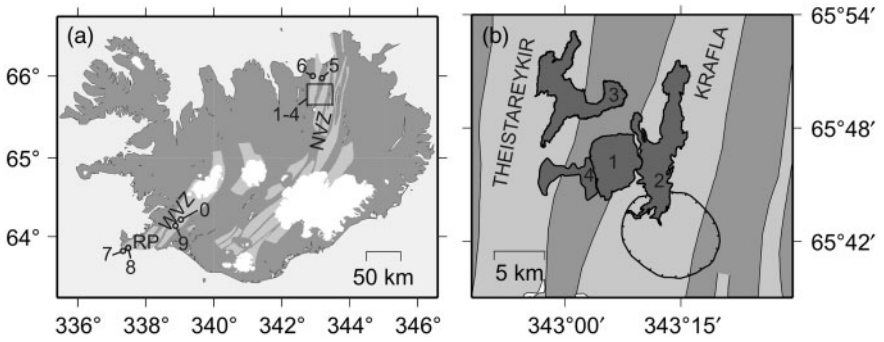

Fig. 1. Map of Iceland showing locations of eruptions with available melt inclusion data. The eruptions are labelled according to the key in Table 1. (a) Light grey zones show the extent of the volcanic systems in the active rift zones. RP, Reykjanes Peninsula; WVZ, Western Volcanic Zone; NVZ, Northern Volcanic Zone. The rectangle marked 1–4 is expanded in (b). Map based on Einarsson & Saemundsson (1987). (b) Detailed map of eruptions from the Krafla and Theistareykir volcanic system. The eruption numbers are placed close to the eruptive vents. (Note the proximity of these vents.) The ring with tick marks shows the position of the walls of the Krafla caldera.

whole-rock analysis were crushed and powdered in an agate shatter-box at the University of Edinburgh. The presence of accumulated phenocrysts in the whole-rock samples means that the whole-rock compositions do not correspond to liquid compositions. Samples for melt inclusion study were hand-crushed and fresh olivines were picked from the crush. These olivines were then optically inspected to identify those containing uncompromised inclusions. Many of the inclusions from Gæsafjöll and several of those from Krafla were naturally quenched to glass. When olivines contained microcrystalline inclusions, they were rehomogenized by heating in an atmosphere fixed at an oxygen fugacity one log unit beneath the fayalite–quartz–magnetite buffer. Gæsafjöll olivines were held at 1240°C and Krafla olivines at 1150°C for 20 min before being quenched by dropping the platinum crucible into a shallow bath of water. After rehomogenization, the olivines and their inclusions were inspected to verify that they were glassy and intact. Olivines containing inclusions were mounted in epoxy and polished until a maximum number of inclusions were exposed. The inclusions were selected for analysis after final inspection under reflected light and back-scattered electron imaging.

ANALYTICAL TECHNIQUES

Whole-rock geochemistry

The concentrations of major elements and selected trace elements in the whole-rock samples were determined by X-ray fluorescence (XRF) at the University of Edinburgh. The protocol of the analyses follows that described by Fitton *et al*. (1998) but the spectrometer used was a Phillips PW2404 XRF with a Rh-anode end-window X-ray tube. The major elements were determined on glass discs, and the traces on powder pellets. Precision and accuracy for the major and trace elements were estimated from repeat runs of standards (BIR1, BHVO1, BCR1) and unknowns. The concentrations of rare earth element (REE) and other trace elements were determined by inductively coupled plasma mass spectrometry (ICP-MS) at the Scottish Universities Environmental Research Centre in East Kilbride following the methods described by Olive *et al*. (2001). Precision and accuracy estimates were gained from multiple repeat measurements of standard BCR1 and unknowns. The precision and accuracy for the REE are better than 1% relative, and for other trace elements better than 5% relative, apart from Rb, Pb and U. The compositions of the whole-rock samples are provided as Supplementary Data, in Electronic Appendix 1, available at http://petrology.oxfordjournals.org/.

Crystal and inclusion compositions

Electron microprobe analysis

The major element compositions of the melt inclusions and their host olivines were determined using the Cameca SX100 electron microprobe at the University of Edinburgh. A range of metal, oxide and silicate (e.g. jadeite, wollastonite) standards were used for calibration of the spectrometers. For olivine analyses, a beam size of 12 μm was used at 20 keV accelerating voltage and a beam current of 20 nA. Accuracy and precision were monitored by repeat analyses of an andradite standard and a St. John's Island olivine standard. Repeats of this olivine standard, which has a similar composition to the samples, gave a relative precision of 0·1% (1σ) for the forsterite content of the olivine, and a relative accuracy of 0·2%. The olivine and melt inclusion compositions are provided as Supplementary Data in Electronic Appendix 2. The major element composition of pillow rim glasses from Gæsafjöll and Stapafell, a subglacial eruption from the Reykjanes Peninsula, were also analysed by electron probe and are presented as Supplementary Data in Electronic Appendix 3.

Ion microprobe analysis

The trace element compositions of the melt inclusions were obtained by secondary ion mass spectrometry (SIMS) on a Cameca IMS-4f ion microprobe at the NERC microanalysis facility at the University of Edinburgh, using a 10 kV primary beam of O^- ions. Positive secondary ions were accelerated to 4500 V, with an offset of 74 ± 5 V to reduce molecular ion transmission. A primary beam current of 5 nA was used, with the beam rastered over a 20 μm area. The raster pit showed well-defined edges and corners for the duration of the analytical work. The following isotopes were analysed by counting for 3 s in each cycle of a 20-cycle run: ^{85}Rb, ^{88}Sr, ^{89}Y, ^{90}Zr, ^{93}Nb, ^{138}Ba, ^{139}La, ^{140}Ce, ^{141}Pr, ^{143}Nd, ^{149}Sm, ^{151}Eu, ^{157}Gd, ^{159}Tb, ^{161}Dy, ^{165}Ho, ^{167}Er, ^{169}Tm, ^{171}Yb and ^{175}Lu. These counts were normalized to ^{30}Si. Because the Si content of the melt inclusions had already been determined by electron microprobe analysis, these values were used in the calculation of absolute elemental concentrations in the melt inclusions. Peak positions were verified before each analysis, and short counts on ^{197}Au (present on the gold coating) were used to reliably determine the peak position at heavy masses. Mass 130·5 was measured as background for 5 s in each cycle and was always zero. FeSi molecular ion interference on Rb was monitored at mass 84 and was negligible. Oxide interference was monitored throughout the analytical session by measurement of ^{154}BaO/Ba and ^{156}CeO/Ce. These oxide–element ratios did not vary systematically with time during the week nor with major or trace element composition of the melt inclusions. Average values for the unknown melt inclusions were $^{154}\text{BaO/Ba} = 0{\cdot}044 \pm 0{\cdot}007$ (1σ) and $^{156}\text{CeO/Ce} = 0{\cdot}213 \pm 0{\cdot}017$. The average ^{156}CeO/Ce can be used to estimate an effective offset voltage of 74 ± 5 V, and this value was used for the calculation of the interference corrections.

The ion yields were assessed every morning by two runs of the NIST standard glass SRM610. These ion yields were then used to calibrate all of the analysed melt inclusion data. These yields did not show any systematic drift during the week of analyses, so an average ion yield was calculated at the end of the week and used to process all of the subsequent data. The precision and accuracy of the analyses were monitored during the week by 14 repeat analyses of glasses of USGS standards BIR01 and BCR01, whose compositions bracketed the observed range of unknown compositions. For analyses of BCR01, precision was better than 3% for Sr, Nb, Zr, Y, La and Ce, 3–10% for the majority of the REE, and 10–20% for Rb, Eu and Lu. Precision estimates for analyses of BIR01 are better than 5% for Sr, Zr, Y and Ba, 5–15% for most of the REE, and 20% for Gd and Lu. The Rb precision is very poor for BIR01. The accuracy of the analyses appears to be similar to their precision. The melt inclusion trace element compositions and the estimated precision and accuracy are given in Supplementary Data in Electronic Appendix 2.

RELATIONSHIP BETWEEN INCLUSIONS AND HOST FLOWS

Significance of phenocrysts, xenocrysts and antecrysts

In subsequent sections, the melt inclusion data are used to constrain melt mixing under Iceland. However, to better understand the significance of these constraints, it is necessary to investigate the relationship between the melt inclusions, their host olivines, and the flow that carries them to the surface. If the host olivines are xenocrysts, whose compositions are unrelated to that of the host flow, then the mixing relationships preserved in the inclusion record provide information about behaviour in the Icelandic crust as a whole. In contrast, if the host olivines are genetically related to their carrier flow, the melt inclusion mixing record can be tied to the processes that occurred within the magmatic plumbing system of the flow. If this second case holds true, where the inclusions' compositions are linked to those of the host flow, then the mixing behaviour can be better constrained in temporal terms.

The following discussion will centre upon the relative incidence of host olivines as equilibrium phenocrysts, xenocrysts or antecrysts (Davidson *et al.*, 2007). Equilibrium phenocrysts are crystals that are in chemical equilibrium with the melt that carries them and xenocrysts are accidental incorporations from older wallrock. Crystals that formed within the plumbing system of the eruption of interest but are not in chemical equilibrium with the carrier melt at the time of eruption are loosely defined as antecrysts (Davidson *et al.*, 2007). The disequilbrium between the antecryst and the carrier melt may form if melt mixing or fractional crystallization occurs after the beginning of crystallization of any part of the eventual antecryst. This compositional disequilbrium will be preserved if the crystal is held in the final carrier melt for a timescale that is short compared with that required for diffusional equilibration. A case of particular importance for Iceland is that where olivines crystallize from melts with a range of compositions, which subsequently mix and erupt before the crystal cargo of original olivines can reach diffusive equilibrium with the mixed melt composition. As noted above, it is seldom possible in practice to distinguish between these crystal types by optical inspection of the samples used in this study. Even when compositional data are available, which may be used to ascertain the possibility of chemical equilibrium between the crystal and the host melt, the classification of a single crystal as an equilibrium phenocryst, accidental xenocryst or antecryst is difficult. Furthermore, it is not always straightforward to make the distinction between xenocrysts and antecrysts at

spreading ridges because the crustal wallrocks are composed predominantly of young plutonic rocks. Fortunately, as is shown in the following section, the large range of trace element compositions in Icelandic lava flows and the widespread occurrence of olivine-hosted melt inclusions in these flows can be used to constrain the genetic relationship between the phenocrysts and the liquids that carry them to the surface.

Trace element compositions

Rare earth element concentrations

Rare earth element (REE) data are available from a number of melt inclusions and whole-rock or glass samples from the eruptions listed in Table 1. The compositions of melt inclusions and host sample whole-rock compositions from Borgarhraun and Gæsafjöll, the most comprehensively sampled eruptions, are shown in Fig. 2, along with the compositions of four further eruptions. The Borgarhraun data consist of 94 melt inclusion analyses and 70 whole-rock analyses (Maclennan *et al*., 2003*a*, 2003*b*) and those for Gæsafjöll consist of 67 melt inclusion and 27 whole-rock analyses. Melt inclusion compositions are always more variable than those of their host melts. However, the average of the melt inclusion compositions is similar to that of the host flow. These relationships are particularly clear for Borgarhraun and Gæsafjöll, possibly because of the large number of samples available. It is notable that the average whole-rock REE concentrations in Borgarhraun are ~10% higher than those of the average melt inclusion. Nevertheless, the REE slopes and therefore ratios of REE to each other are very similar. This relationship indicates that the difference in REE concentration between the average of the Borgarhraun melt inclusions and that of the whole-rock is likely to be caused by fractional crystallization, because the slope of the REE and REE ratios such as La/Yb are not significantly influenced by moderate amounts of fractional crystallization of the phases found as phenocrysts or in cumulate xenoliths in Icelandic rift zone basalts (Maclennan *et al*., 2001a, 2003*b*; Gurenko & Sobolev, 2006; Holness *et al*., 2007).

REE and other trace element ratios

The close correspondence in the average REE compositions of the melt inclusions to that of the carrier lava is also evident in Fig. 3. The small filled circles in Fig. 3a show the average La/Yb of the melt inclusions plotted against that of the host lava for the 10 eruptions of Table 1. It should be noted that the averages are calculated as $\sum$La/$\sum$Yb, and, because all samples were analysed for La and Yb, this average is equal to the $\overline{\text{La}}/\overline{\text{Yb}}$. The significance of this calculation is that if each melt inclusion represents a sample of an equal volume of melt, then mixing of these melt volumes will produce a final melt with a La/Yb equal to $\overline{\text{La}}/\overline{\text{Yb}}$ of the inclusions. These data lie close to the 1:1 correspondence line indicated on the plot, with the exception of Mælifell, Miðfell and the

Table 1: Host lava flows for melt inclusions

Eruption	Ref.[1]	Zone[2]	Map[3]	Age[4]	N[5]	Fo_{av}[6]	$(La/Yb)_{av}$[7]	$\bar{X}_e$[8]	σ_{X_e}[9]	P_{max}[10]	P_{min}
Gæsafjöll	1	N	1	G	67	83·3	2·99	0·63	0·12	0·76	−0·49
Krafla	1	N	2	R	8	78·8	2·12	0·46	0·09	0·23	−0·28
Borgarhraun	2, 3, 4	N	3	P	94	89·2	0·89	0·19	0·54	1·34	−0·47
Bóndhólshraun	2	N	4	P	10	89·0	1·40	0·30	0·12	0·37	−0·40
Langavíti	2	N	5	P	12	90·4	1·04	0·22	0·15	0·77	−0·46
Picrites	2	N	6	P	7	89·6	1·18	0·25	0·18	0·66	−0·58
Háleyjabunga	5, 6	R	7	P	14	89·9	0·63	0·12	0·16	1·41	−0·37
Stapafell	6	R	8	G	9	85·2	3·19	0·66	0·18	0·72	−0·55
Mælifell	5	W	9	G	7	88·9	3·69	0·37	0·45	1·31	−0·76
Miðfell	5	W	0	G	15	88·5	1·86	0·37	0·44	1·29	−0·77

[1]Data sources for melt inclusion and host olivine compositions. 1, This study; 2, Slater *et al*. (2001); 3, Maclennan *et al*. (2003*a*); 4, Maclennan *et al*. (2003*b*); 5, Gurenko & Chaussidon (1995); 6, Maclennan (2008).
[2]Rift Zone. N, Northern Volcanic Zone; R, Reykjanes Peninsula; W, Western Volcanic Zone.
[3]Key for map in Fig. 1.
[4]Age of flow. G, subglacial eruption, >14·5 ka; P, early postglacial eruption, between 14·5 ka and 7 ka; R, recent eruption, younger than 7 ka.
[5]Number of olivine-hosted melt inclusions analysed from each eruption.
[6]Average forsterite content (molar per cent) of the olivine hosts to the inclusions.
[7]Average La/Yb of the melt inclusions from the flow.
[8]Average X_e of inclusions (see text for details of calculation).
[9]Standard deviation of X_e from inclusions in flow.
[10]Maximum and minimum of P in inclusions from the flow (see text for details of calculation).

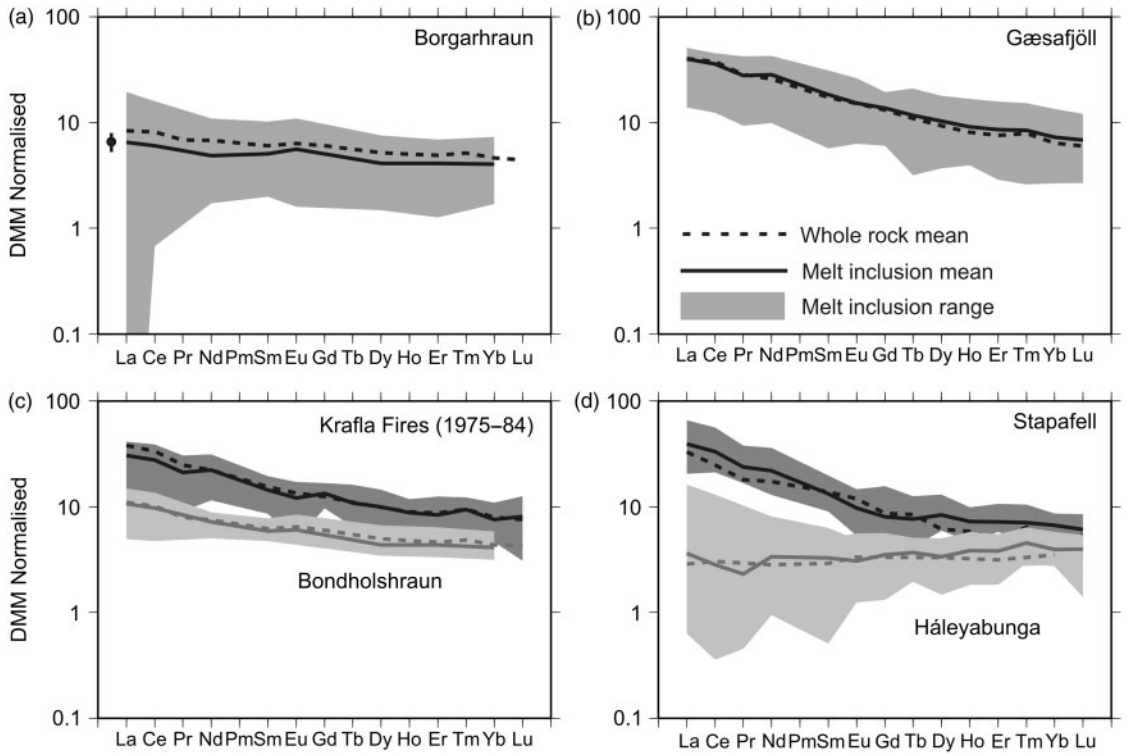

Fig. 2. Rare earth element (REE) data for melt inclusions and their host eruptions. All concentrations are normalized to the depleted MORB mantle (DMM) source composition of Workman & Hart (2005). Grey field shows range of inclusion compositions within each eruption. Dashed line shows the average of melt inclusion compositions in the eruptions. Continuous line shows the average of whole-rock or glass compositions from the eruptions. The small diamond in (a) gives an estimate of the standard error of estimation of the average of the melt inclusion compositions.

Theistareykir picrites, which have higher La/Yb in the melt inclusion average than in the whole-rock. It has recently been proposed that percolation of melt through gabbroic mush controls the trace element composition of the Miðfell melts, in particular the behaviour of Sr (Gurenko & Sobolev, 2006). However, such percolation has a limited effect on the La/Yb ratios and leads to slight increases in the La/Yb of the percolating melt. It is therefore unlikely that percolation is responsible for the apparent difference in the average compositions of the Miðfell melt inclusions and carrier melt. When comparing the average of the melt inclusion data with that of the whole-rock it is useful to consider the quality of these estimates of the means. Errors in the estimate of the average of a population are controlled by the natural variation within the population, commonly quantified using the standard deviation, σ, and the number of samples used to estimate the mean, N. The standard error of estimate of the mean is given by $S_E = \sigma/\sqrt{N}$. Table 1 shows that the REE variation in Mælifell and Miðfell is almost as large as that found in Borgarhraun, whereas the number of samples used to estimate the mean is ~10 times smaller. The accuracy of analytical techniques must also be taken into account when comparing averages derived from SIMS, ICP-MS and laser ablation (LA)-ICP-MS techniques. The error ellipses in Fig. 3a reflect the combination of $1S_E$ and the accuracy of the measurements. The plotted $1S_E$ error ellipses for six of the flows intersect the 1:1 line. If $2S_E$ are used then all of the flows intersect the 1:1 line. Therefore, within error, the average La/Yb ratios of the melt inclusions are the same as those of their host flows. The apparent discrepancy for Mælifell, Miðfell and the Theistareykir picrites may reflect insufficient sampling of heterogeneous populations.

The same procedure can be applied to other trace element ratios that are strongly influenced by mantle processes but relatively insensitive to processes in the Icelandic crust. If Sm/Yb is considered in the same way, then eight out of the 10 eruptions have mean whole-rock compositions within $1S_E$ of the mean melt inclusion composition. This agreement is better than expected for errors from a Gaussian distribution, where ~70% of the flows would be expected to agree within $1S_E$. The poorer fitting flows in this case are Mælifell and Stapafell. For Zr/Y, seven out of the 10 flows have mean whole-rock and mean melt inclusions that plot within $1S_E$, with Bondhólshraun, Miðfell and Gaesafjöll out of agreement. For Nb/Y, where fewer data is available, four out of six flows are in agreement, with only Háleyjabunga and Miðfell having melt inclusion and whole-rock means that differ by more than $1S_E$.

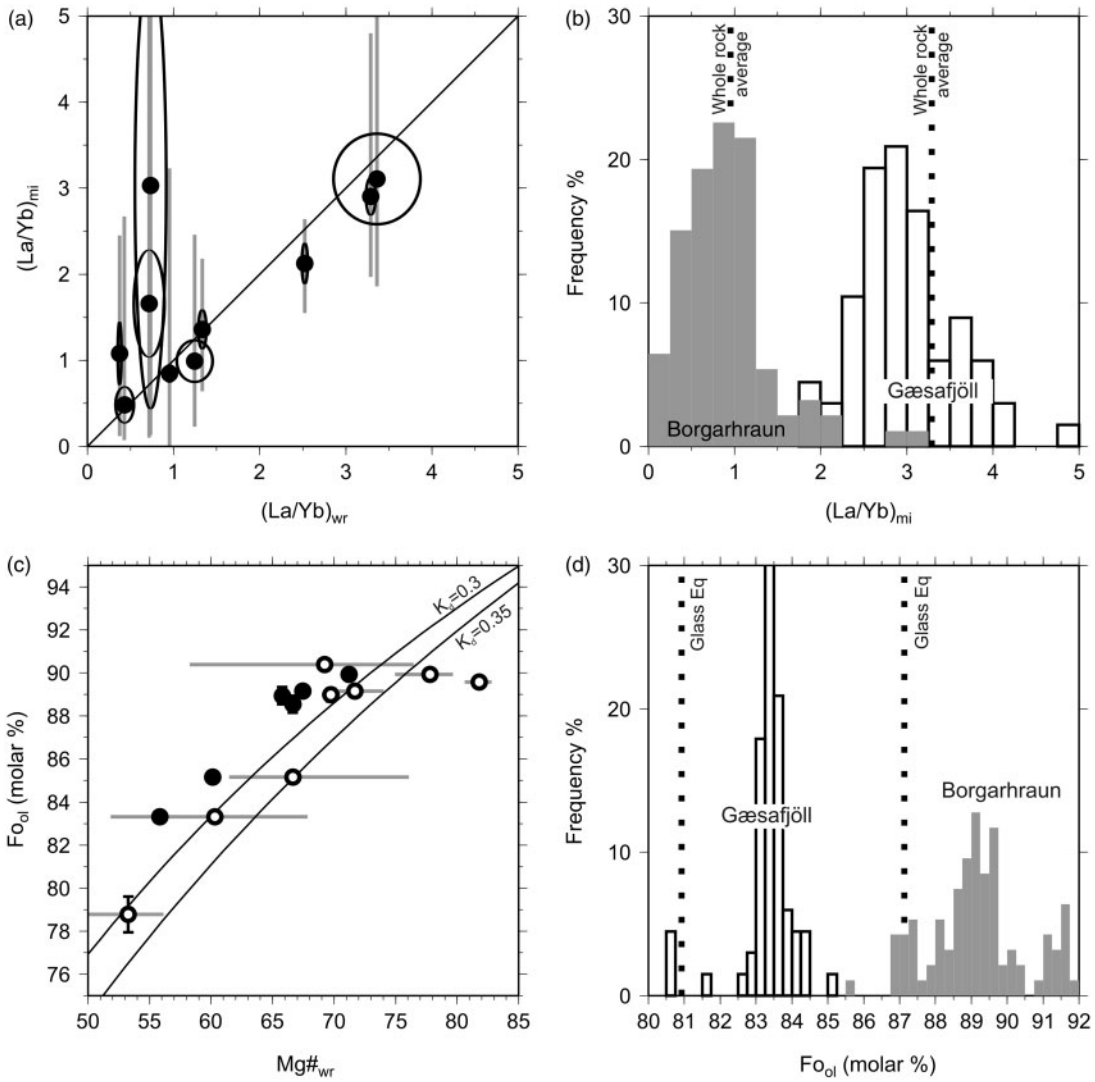

Fig. 3. Compositional relationships between melt inclusions, host olivines and host lava flows. (See text for further details.) (a) Small filled circles show mean La/Yb for melt inclusions (mi) plotted against mean La/Yb for host-rock samples (whole-rock; wr) for the 10 flows listed in Table 1. The grey bars show the total compositional range from the inclusions in each flow. The error ellipses show the 1σ standard error of estimate of the means. (b) Histograms of melt inclusion compositions from Borgarhraun, grey filled bars, and Gæsafjöll, fine black outlined bars. The average compositions of the whole-rock samples are shown as dotted vertical lines. (c) Small filled circles show average composition of olivine crystals (Fo mol%) in each eruption plotted against the composition (Mg-number) of glass. The vertical error bars are 1σ standard error of estimate of the means for the olivine. Grey bars show range of whole-rock Mg-numbers, with the open circles showing the average. (d) Histogram of olivine compositions from Borgarhraun (grey filled bars) and Gæsafjöll (fine black outlined bars). The composition of olivine in equilibrium with the host glass, assuming a K_d^{Fe-Mg} of 0·3, is shown by the vertical dotted lines.

The concurrence of the estimated mean of the melt inclusions with that of the whole-rock of the carrier flow is as expected given the statistics of the standard error of estimate of the mean. Further evidence for this statistical agreement comes from the observation that different eruptions lie outside $1S_E$ for different element pairs.

In contrast, the behaviour of elemental concentrations or ratios that are strongly influenced by crustal processes such as fractional crystallization or crystal accumulation do not show good agreement between melt inclusion and whole-rock means from individual eruptions. For example, only three out of 10 eruptions show agreement within $1S_E$ for Sr/Nd, with six eruptions having higher Sr/Nd in the whole-rock mean than in the melt inclusions. These eruptions all contain plagioclase phenocrysts, and the high Sr/Nd of the whole-rock mean compared with the melt inclusion mean is likely to result from plagioclase accumulation. This accumulation will also cause a mismatch for elements such as Ca and Na.

The Theistareykir picrite flow has a melt inclusion mean Sr/Nd that is higher than that of the host lava. This high mean is partly due to the presence of two inclusions with large positive Sr anomalies. More generally, 11 inclusions out of the 203 with available Sr/Nd from the dataset have large positive Sr anomalies, with Sr/Nd >50. These inclusions may correspond to melts that have interacted with plagioclase in the crust prior to their entrapment (Danyushevsky *et al.*, 2004; Gurenko & Sobolev, 2006). Further consideration of the possible role of such crustal processes is provided in the discussion section of this paper. However, it is worth noting at this stage that the correlation between Sr/Nd and trace element ratios such as La/Yb, Sm/Yb, Nb/Y or Zr/Y is very weak, and that removal of the inclusions with large positive Sr anomalies from the dataset does not influence the conclusion that incompatible element ratios that are variable in mantle melts and little altered by processes in the Icelandic crust show good agreement between the mean composition of the melt inclusions and the mean composition of the whole-rock samples of the host flow.

Compositional distribution in closely spaced eruptions

The vertical grey bars in Fig. 3a indicate the total range of melt inclusion compositions measured from each eruption. Early postglacial eruptions from the Theistareykir volcanic system, such as Borgarhraun, Bóndhólshraun, Langavíti and the Theistareykir picrites, show large and overlapping ranges in melt inclusion distributions. Despite this extensive compositional overlap in the melt inclusion distributions, the well-constrained means of the distributions from Borgarhraun and Bóndhólshraun are different, and correspond to the whole-rock means. Primitive subglacial eruptions, such as Gæsafjöll, also show a large range in melt inclusion compositions, but have limited overlap with the compositional range found in the early postglacial eruptions. The detailed map in Fig. 1 shows that the distance between the eruptive vents for Gæsafjöll and Bóndhólshraun is less than 5 km. In fact, the Bóndhólshraun crater is situated in a gully on the western flanks of the older Gæsafjöll eruption. Although the vent sites of these two eruptions lie close to each other, the deeper magmatic plumbing systems appear to have been physically separated: the distribution of melt inclusion compositions is different, and, most strikingly, the maximum La/Yb of any measured inclusion from Bóndhólshraun is significantly lower than the mean La/Yb from the Gæsafjöll inclusions. This apparent separation of the deeper plumbing system of closely spaced eruptions is also clear from the other eruptions shown in Fig. 1b. The vents of Borgarhraun, Bóndhólshraun, Gæsafjöll and the Krafla fissure eruptions are found within a circle of 12 km diameter, but have average melt inclusion compositions that are distinct.

The distributions of melt inclusion compositions from the densely sampled and closely spaced Borgarhraun and Gæsafjöll eruptions are unimodal (Fig. 3b). The modes of the distribution of La/Yb in melt inclusions from the two flows lie close to that of the average of the whole-rock samples. These unimodal and different distributions are not expected to occur if the olivine hosts to the melt inclusions are accidental xenocrysts incorporated either from unrelated wall-rock at the margins of a single magma chamber or randomly from the Icelandic crust.

Constant average REE ratios with varying host olivine composition

One further observation provides useful constraints upon the relationship between the inclusions and the host flow. Whereas the variability in the REE concentrations and ratios of Borgarhraun melt inclusions has been shown to drop with decreasing forsterite content of the host olivine, the average of the REE ratios, such as La/Yb, remains near constant in olivines with <90% molar forsterite (Maclennan *et al.*, 2003*a*, 2003*b*). The near-constant average La/Yb is similar to that of the Borgarhraun whole-rock average. This observation has been used as evidence of concurrent mixing and crystallization of batches of compositionally diverse, primitive melts in the plumbing system of Borgarhraun (Maclennan *et al.*, 2003*a*).

Mg–Fe partitioning and olivine compositions

It is possible to examine the relationship between the olivine phenocrysts and their carrier melts by comparing the observed partitioning of Mg and Fe between the crystal and its host melt with the behaviour expected under conditions of chemical equilibrium. Compilations and parameterizations of experimental data indicate that the value of K_d^{Fe-Mg} is expected to be 0·31 for melts of Icelandic composition and is likely to lie within the range $0{\cdot}3 < K_d^{Fe-Mg} < 0{\cdot}35$ (Ford *et al.*, 1983; Putirka, 2005). Both direct observation (Oskarsson *et al.*, 1994) and use of experimental parameterizations (Kilinc *et al.*, 1983) indicate that approximately 10% of the Fe in Icelandic basaltic melts is present as Fe^{3+}. Glass compositions were available from six of the eruptions; from pillow rims, tephra or glassy margins of subaerial flows. All of these glass compositions have Mg-number [molar $Mg/(Mg + Fe^{2+})$] too low to be in equilibrium with the mean olivine compositions from the flows. The range and mean of whole-rock sample Mg-numbers are also displayed in Fig. 3c. These whole-rock compositions are influenced by the accumulation of olivine and, more rarely, clinopyroxene crystals in the melt. Nevertheless, eight out of the 10 eruptions show a minimum whole-rock Mg-number that is too low to be in equilibrium with the mean olivine in the flows. These samples with minimum Mg-numbers are likely to contain the fewest accumulated crystals and, where glass compositions are absent, give the best estimate of the carrier melt composition. For two eruptions, the picrites from Theistareykir

and Háleyjabunga, the Mg-numbers of the whole-rocks are higher than those expected for equilibrium with the average olivine composition of the flow. However, all of the available samples from these picrites contain significant quantities of accumulated olivine crystals.

The histograms of Fig. 3d serve to further illustrate the relationship between the olivines and the host flows. The modes of both the Borgarhraun and Gæsafjöll olivines are too forsteritic to be in equilibrium with the glass in tephra or pillow rims from these eruptions. However, both of the eruptions contain a small cluster in olivine compositions close to the expected equilibrium composition. The trace element data, presented in a later section, indicate that the melt inclusions contained in these relatively low forsterite content phenocrysts have a rather limited range of melt inclusion trace element compositions, close to the average composition of the host flow.

Summary

The observations described above indicate that 90% or more of olivine phenocrysts present in the eruptions studied are too forsteritic to be in equilibrium with their carrier magma. However, the relationship between the trace element compositions of the melt inclusions and those of the whole-rock samples demonstrates that the olivines are not accidental xenocrysts. It is therefore likely that the olivines grew from a suite of parental melts that mixed to form the liquid that transported the crystals to the surface. Initially, primitive mantle melts with variable trace element compositions are supplied to magma bodies where they start to crystallize. This crystallization produces forsteritic olivines and these olivines entrap melt inclusions with a wide range of trace element compositions. Next, the diverse melt compositions mix together and this mixing homogenizes the trace element composition of the host melt. As the mixing melt sits in magma bodies, it continues to cool and crystallize, forming progressively less forsteritic olivines. However, the early formed forsteritic olivines that host the melt inclusions are retained in or re-entrained into the evolved, mixed carrier melt, which transports the olivines to the surface for eruption. The cores of such olivines are commonly out of Mg–Fe equilibrium with surrounding glass, and exhibit short (20–50 μm) normal zoning profiles at their margins. When compositions are available for host glasses, they are close to Mg–Fe equilibrium with the margins of the olivines. All of the analysed melt inclusions are taken from within the unzoned cores of the olivines, and the relationship between the host olivine and melt inclusion compositions do not reflect the processes that cause the zonation. As described in a later section, these observations indicate a timescale of decades or less between entrainment of the olivines in the final melt composition and their eruption. In the terminology of Davidson *et al.* (2007), such crystals may be described as antecrysts.

If the above model is correct then study of the melt inclusion and olivine compositions can be used to investigate mixing and crystallization in the roots of the eruption that hosted them. The remainder of the paper will therefore focus on the characterization of these processes under Iceland.

QUANTIFICATION OF MIXING OF MELTS

Mixing end-members and extent of crystallization

When quantifying the extent of mixing it is useful to make the simplifying assumption that mixing takes place between two end-member parental melts, one enriched in composition, and the other depleted. Although this assumption is not likely to be correct in detail, with progressive fractional melting of a heterogeneous source possibly playing a role in generating a wide range of primary melt compositions, study of the relationship between the isotopic and trace element composition of Theistareykir basalts indicates that over 90% of the trace element variation can be accounted for by mixing between melts from two sources. Similar results have recently been obtained for Reykjanes whole-rock and melt inclusions (Maclennan, 2008). The supply of an apparently bimodal population of melt compositions to the deep magma bodies where olivines trap melt inclusions may result from channelized flow of melt in the mantle (Maclennan, 2008).

The composition of suitable end-member melts can be estimated from the extreme compositions present in the melt inclusion population from all Icelandic rift zone samples (Electronic Appendix 2). The melt inclusions are all from rift zone eruptions, and comparison of whole-rock and melt inclusion data from Theistareykir–Krafla, the Reykjanes Peninsula and Mælifell–Miðfell on the Western Rift Zone indicate that the range of trace element compositions present in each area is similar and that the extreme compositions of melts fed from that the mantle to deep magma bodies does not vary greatly across the parts of the rift zones included in this study. Models of the effect of deglaciation on mantle melting under Iceland, which have been successfully applied to temporal variation in the average REE composition of basalts from Theistareykir and Krafla, predict no variation in the total range of instantaneous fractional melt compositions produced in the mantle during the deglaciation cycles. The changes in the average composition are in this case achieved by changing the weighting of the fractional melts generated at different depths. Therefore, as a first approximation, we use the same extreme melt inclusion compositions to quantify the mixing of melts prior to both glacial and postglacial eruptions. The method should not be applied to melt inclusions

from the flank zones of Iceland, where the presence of transitional and alkaline basalts indicates that the top of the melting region is at greater depth and that the maximum melt fraction attained is smaller than under the rift zones. In these flank regions, it is likely that the extreme depleted compositions will be less depleted than those found under the rift zones.

Once the end-member compositions have been defined it is possible to determine the fraction of the enriched end-member melt, X_e, present for any melt inclusion or whole-rock composition. In binary mixing, the fraction of depleted end-member melt, X_d, is equal to $1-X_e$. The advantage of using the binary mixing simplification is that for any fully mixed melt batch, the variance of the initial melts in the unmixed batch is given by

$$\sigma_0^2 = X_e(1 - X_e).$$

A suitable indicator of the degree of mixing within the batch is then given by

$$M = 1 - \left(\frac{\sigma^2}{\sigma_0^2}\right)$$

where σ^2 is the compositional variance of the partially mixed batch of melt and the mixing parameter, M, rises from zero when no mixing has taken place to unity when mixing is complete (Danckwerts, 1953). The evolution of mixing of two extreme melt compositions is shown in schematic form in Fig. 4.

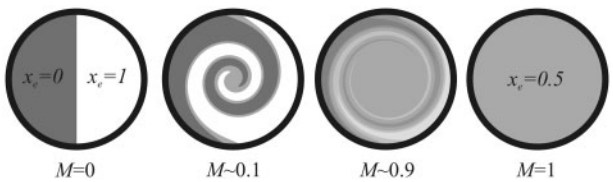

Fig. 4. The evolution of mixing of a passive tracer, following the logic of Danckwerts (1953) with four stages of mixing shown. The extent of mixing increases from left to right, as indicated by variation in the parameter M beneath each snapshot. The chamber is a closed system, and the average composition of the liquid in the chamber remains at $\bar{X}_e = 0{\cdot}5$. Initially, two extreme melt compositions are physically juxtaposed in the chamber. Half of the chamber is composed of melt with $X_e = 0$, the depleted end-member, and the other half is composed of melt with $X_e = 1$, the enriched end-member. The initial variance and extent of mixing can be calculated as described in the text. At this stage of physical juxtaposition, the value of the mixing parameter, M, is zero. The snapshot at $M \sim 0{\cdot}1$ demonstrates the effect of the mechanical rearrangement of the compositional heterogeneities by stirring. This rearrangement may occur as a result of convective motions within the chamber. In this case, little diffusion has taken place, and only a thin strip of material at the boundary between the two regions has a composition of $X_e \sim 0{\cdot}5$. The next snapshot, at $M \sim 0{\cdot}9$, shows the effect both of continued stretching and thinning of heterogeneities by stirring and partial homogenization by diffusion. The plot on the right shows the distribution of melt compositions after mixing is complete and $M = 1$. Once stirring has thinned the regions of melt with distinct compositions to a sufficiently small length scale, diffusion is able to homogenize the melt composition to the molecular scale. In this case, all the melt in the chamber has the composition of the chamber average, at $X_e = 0{\cdot}5$.

The X_e values were estimated for each melt inclusion and whole-rock composition using the REE concentrations. Because the sample compositions have been influenced by fractional crystallization in addition to mixing, it is necessary to generate a forward model for composition that includes both X_e and F, the average extent of crystallization, as follows:

$$C = \left[\frac{X_e C_e}{1 - F_e} + (1 - X_e)C_d\right](1 - F)^{D-1}.$$

The variable F_e was introduced to account for possible differences in the relative degree of crystallization or host–olivine interaction in the two compositional end-members. It was assumed that the effective partition coefficient for these processes was zero. However, for the subsequent fractional crystallization through the interval F, bulk partition coefficients D were calculated from estimates of the modal mineralogy of the crystallizing solid and the partition coefficients of each of these solid phases. The modal mineralogy of the solid was assumed to be similar to that of the gabbroic material found to best fit the major element trends of samples with <9·5 wt % MgO from the Krafla and Theisteraykir volcanic systems (Maclennan *et al.*, 2001*a*). Suitable partition coefficients for minerals from these systems were calculated using the approach of Wood & Blundy (1997) for clinopyroxene, Bindeman *et al.* (1998) for plagioclase and Bédard (2005) for olivine. Typical bulk partition coefficients are therefore $D_{La} = 0{\cdot}08$, $D_{Sm} = 0{\cdot}10$ and $D_{Yb} = 0{\cdot}11$. The misfit function between predicted and observed compositions is defined as

$$\Theta = \sum_{i=1}^{N} (C_i^{obs} - C_i^{calc})^2 + W(R^{obs} - R^{calc})^2$$

with R^{obs} and R^{calc} referring to the observed and calculated La/Yb ratio of the sample. The weighting factor, W, was set to 100 to ensure that recovered X_e were controlled by the trace element ratios that are not strongly sensitive to crustal processes. This misfit function was minimized by varying X_e, F_e and F using the amoeba subroutine described by Press *et al.* (1992). To allow comparison between whole-rock and melt inclusion data, only the elements La, Ce, Sm, Nd, Dy, Er and Yb were used in the minimization, as these elements are available from almost every inclusion analysed by ion probe.

The results of fits to typical melt inclusion compositions from the Borgarhraun and Gæsafjöll eruptions are shown in Fig. 5. Comparison of the La/Yb and X_e of Borgarhraun inclusions in Fig. 6 confirms the strong correlation between these quantities ($r = 0{\cdot}99$). Other trace element ratios that are thought to be largely unaffected by fractional crystallization or crustal melting under Iceland, such as Sm/Yb, also correlate well with X_e ($r = 0{\cdot}95$).

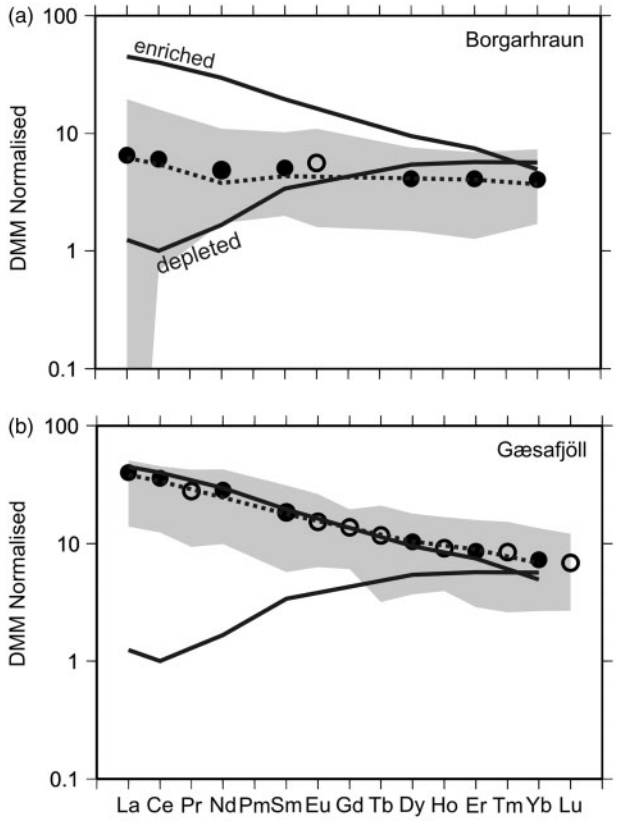

Fig. 5. Plot showing extreme melt inclusion compositions chosen as end-members to convert REE compositions into X_e. The end-members have the maximum and minimum Sm/Yb ratios amongst the inclusions. If the inclusion with extremely low La concentrations is used as the depleted end-member then the fits to the rest of the inclusion data are degraded, but the returned X_e are similar. The circles show the composition of a selected inclusion, with the error bars showing the 1σ precision. These error bars are smaller than the size of the symbol. Filled circles show elements that were used in the fitting, whereas open circles were not included in the misfit calculations. The result of the fit is shown as the black dashed line. Inclusions from both depleted and enriched eruptions are well matched by the fitting procedure.

The modelled extent of fractional crystallization, F, correlates with the forsterite content of the olivine host of the melt inclusion ($r = -0{\cdot}70$), indicating that the fit has not only successfully recovered the proportion of the mixing end-members but also the progression of crystallization. The root-mean-square (r.m.s.) of the error in the fit normalized to the 1σ analytical precision has an average of 0·69, with 84% of the fits having an r.m.s. <1. The success of the fitting procedure to the seven REE, which is controlled by two variables alone, is expected from principal component analyses of the dataset of all available Icelandic inclusions, which show that over 98% of the variance in these elements can be accounted for with just two principal components. The first component reflects variations in concentrations, and the second tracks fractionation of the light REE (LREE) from the heavy REE (HREE). The application of principal component analysis to whole-rock samples and melt inclusions from Iceland has been thoroughly described in a number of studies and these found similar trace element behaviour (Slater *et al.*, 2001; Maclennan *et al.*, 2003*a*, 2003*b*).

Inclusions in a single flow

The Borgarhraun lava flow from the Theistareykir volcanic system of northeastern Iceland has been the focus of intensive sampling, and a large dataset of whole-rock and melt inclusion analyses is available from this flow (Slater *et al.*, 2001; Maclennan *et al.*, 2003*a*, 2003*b*). The relationship between the variation of the trace element composition of the inclusions and the forsterite content of their olivine hosts is consistent with the concurrent cooling and mixing of melts in the plumbing system of this flow (Maclennan *et al.*, 2003*a*). The results of application of the method of quantification of mixing described above are shown in Fig. 6. An important difference between these results and those of Maclennan *et al.* (2003*a*) is that the present assumption of binary mixing allows quantification of the total progression of mixing after melts with the composition of the end-members were brought into physical contact.

The most striking feature in Fig. 6 is the drop in the variation of La/Yb and X_e and the corresponding rise in M over the interval from 90% to 86% forsterite in the host olivine. The drop in the forsterite content of the olivines records the progression of cooling and crystallization of the batches of melt. The decrease in the variation of X_e tracks the extent of compositional homogenization by mixing of melts. It is worth noting that X_e is unaffected by crystallization and, like La/Yb, acts effectively as a passive tracer of the mixing. The variance of X_e and the corresponding M were calculated in a sliding window in forsterite content with a window width of 1% forsterite. The quality of the estimate of M is dependent on the number of samples available in each window. The 95% confidence limits on the calculation of M were therefore calculated using the χ^2 distribution as described by Maclennan *et al.* (2003*a*). The data provide robust evidence for mixing in the crystallization interval corresponding to the drop in forserite content from Fo_{90} to Fo_{86}. The relationship between M and the molar per cent forsterite content of the host olivines can be approximated by $dM/dFo \approx 0{\cdot}03$ per mol %. The data indicate that mixing and cooling are concurrent under Theistareykir, and Maclennan *et al.* (2003*a*) have suggested that this behaviour may reflect the action of convection in magma chambers.

A different type of behaviour is recorded by melt inclusions that are hosted in olivines with between 90 and 92% molar forsterite. These inclusions show a decrease in M with decreasing forsterite content. This relationship is likely to arise from the supply of mantle melts with varying compositions into the magma chambers where

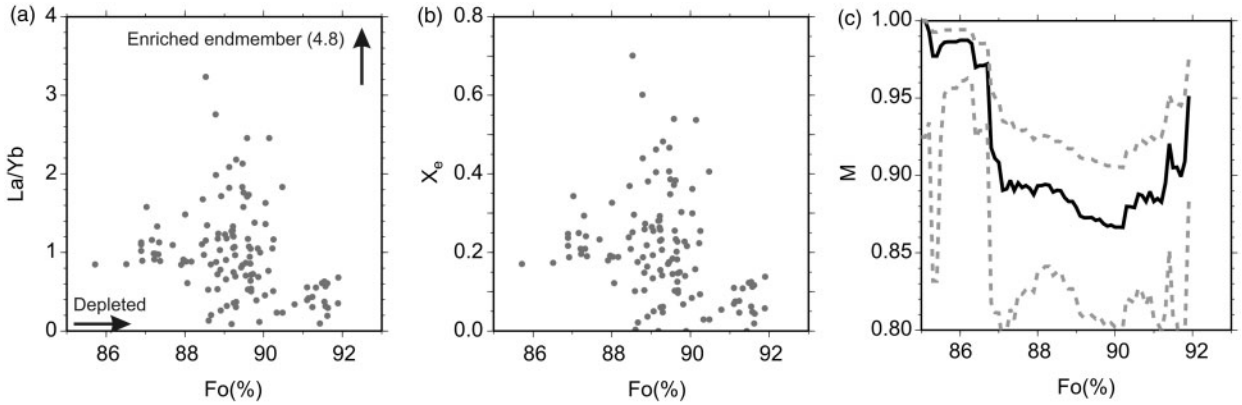

Fig. 6. The record of concurrent mixing and crystallization in melt inclusions from Borgarhraun. (a) Grey circles show La/Yb of melt inclusions plotted against the forsterite content (mol %) of their host olivine. The arrows indicate the compositions of the extreme depleted and enriched end-member compositions used in the conversion to X_e. (b) Plot of X_e, the fraction of enriched end-member, in each inclusion plotted as a function of host forsterite content. The similarity of the distribution of compositions in (a) and (b) should be noted. (c) Evolution of the mixing parameter, M, as a function of olivine composition is shown as the continuous black line. This parameter was calculated by obtaining the standard deviation of inclusion X_e over a window of width 1 mol % forsterite. The quality of the estimate of the standard deviation is controlled by the number of samples available in each window. The 95% confidence limits on M are therefore calculated using the χ^2 as described by Maclennan *et al.* (2003*b*) and shown as dashed grey lines.

crystallization occurs (Maclennan *et al.*, 2003*a*). Mantle melts produced in the deepest parts of the melting region are predicted to have higher La/Yb and lower Mg/Fe than those from the shallower parts of the melting region. Therefore, the melts with the lowest La/Yb and X_e can be entrapped only in the most forsteritic olivines, Fo_{92}, because these olivines grow from melts with the highest Mg/Fe ratio. Melts in equilibrium with Fo_{90} olivine may be either unmodified melts from the deeper parts of the melting region or shallow mantle melts that have lost a small proportion of their mass through fractional crystallization. Therefore, the maximum range in melt La/Yb is available for entrapment in Fo_{90} olivines, whereas only the most depleted part of this distribution can be entrapped in Fo_{92} olivines.

All Icelandic melt inclusions

When the extent of mixing, M, is calculated for melt inclusions within single eruptions, and plotted as a function of the average forsterite content of the olivines in the eruptions, then a crude increase in the extent of mixing can be observed with decreasing Fo. However, when confidence limits on M are calculated, the eruptions with limited number of observations available (<10) show large uncertainty in M. It is therefore preferable to use all of the available melt inclusion compositions, and establish the relationship between M and host olivine composition. Because different eruptions have different average compositions, it is useful to define the following indicator of variability:

$$P^k = \frac{X_e^{i,j} - \bar{X}_e^j}{\sqrt{\bar{X}_e^j(1-\bar{X}_e^j)}}$$

where $X_e^{i,j}$ is the fraction of the enriched end-member in the ith inclusion in the jth eruption, and $\bar{X}_e^j$ is the average fraction of the enriched end-member in samples from the jth eruption. This parameter P therefore gives the difference between a sample composition and the average of the eruption that it comes from, normalized to the expected standard deviation of the unmixed original volume of depleted and enriched end-member melts for that eruption. The index k associated with P refers to the kth inclusion in the dataset of inclusions of interest, which may come from several flows. Using P it is therefore possible to compare the evolution of compositional variation with host olivine composition simultaneously for a number of different eruptions.

It follows that to calculate M for the $k=1, \ldots, N$ samples the following expression may be used:

$$M = 1 - \frac{\sum_{k=1}^{N} P_k^2}{N}.$$

A further advantage of the use of P is that it overcomes the problems that arise as a result of the focused study of melt inclusion variability from a handful of flows, each of which has a different trace element composition. Therefore, before a large number of inclusion compositions are available from many of the flows from the volcanic zones of Iceland, it is necessary to use P.

The results of the calculation of P and the associated M are shown for all available Icelandic melt inclusion compositions in Fig. 7. The dataset of all 243 available Icelandic melt inclusions shows evidence for concurrent mixing and crystallization of melts, similar to that indicated by the

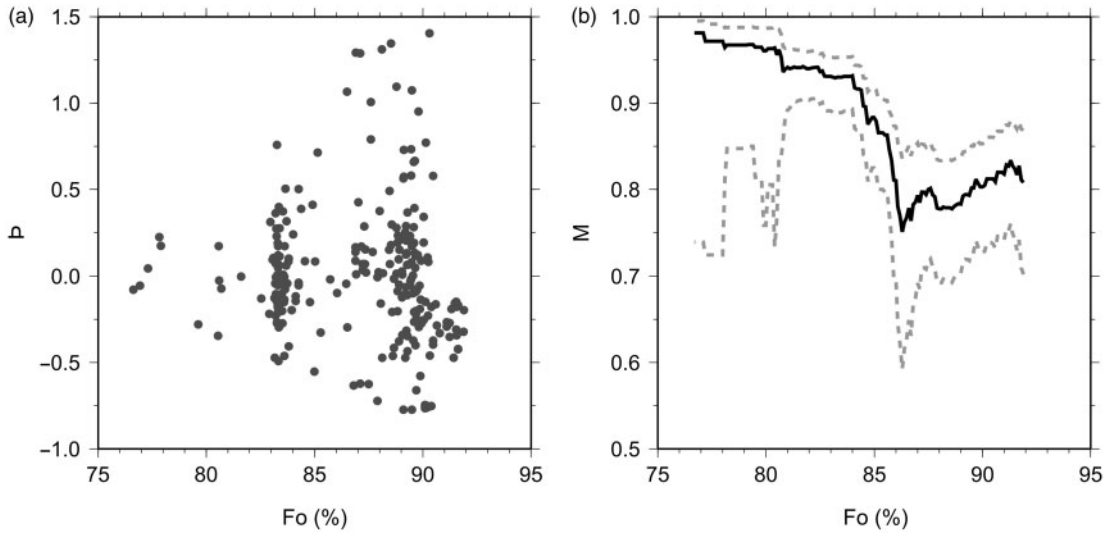

Fig. 7. (a) Evolution of the deviation of melt inclusion composition from the flow average composition as a function of the host olivine composition. Data are taken from all available Icelandic melt inclusion compositions. The deviation of the melt inclusion composition from the average is calculated using the parameter *P* as described in the text. (b) Variation in *M* calculated from the values of *P* in (a) as described in the text is shown as a continuous black line. The window width and 95% confidence limits are shown in the same way as in Fig. 6.

data from Borgarhraun alone. The normalized deviation of the inclusion composition from the flow average, *P*, shows a decrease in its variance with decreasing forserite content of the host olivine. The decrease in the variance of *P* corresponds to an increase in the inferred extent of mixing, *M*, from 0·75 at Fo_{87} to 0·97 at Fo_{78}, with much of the drop in variation occurring close to Fo_{85}. The rate of mixing with respect to change in forsterite content is similar to that observed for Borgarhraun, with d*M*/dFo ≈0·06/mol % between Fo_{87} and Fo_{84} and d*M*/dFo ≈0·02/mol % between Fo_{87} and Fo_{77}. These estimates indicate that the relative rates of mixing and cooling derived for Borgarhraun also apply to Icelandic basaltic magma chambers in general, and that concurrent mixing and cooling is common in magma bodies under Iceland. These results are not dependent on observations from one eruption alone: if Borgarhraun or Gæsafjöll inclusions are removed from the analyses then very similar conclusions are drawn, despite the degradation in quality of the estimates of *M* caused by the smaller number of samples available for its calculation. The dataset of all Icelandic melt inclusions shows a drop in *M* from Fo_{92} to Fo_{87}, showing a similar establishment of variability by the addition of mantle melts to that recorded between Fo_{90} and Fo_{92} in the Borgarhraun dataset.

Whole-rock data

Whole-rock compositional data from the rift zones of Iceland also show evidence for concurrent mixing and cooling of melt. Major and trace element data from the Northern Volcanic Zone and Reykjanes Peninsula are plotted in Fig. 8, and similar patterns are observed in datasets from the Western Rift Zone (Sinton *et al.*, 2005) and central Iceland (Maclennan *et al.*, 2001*b*). In samples with <10 wt % MgO, trace element ratios such as Sm/Yb and Nb/Y show decreasing variation with a drop in the MgO content of the whole-rock samples. These trace element ratios are unlikely to be strongly influenced by fractional crystallization or crustal melting under Iceland and can therefore be used as passive tracers of mixing in the crust. Despite the importance of olivine accumulation in some of the samples with >10 wt % MgO, the evolution of whole-rock MgO broadly reflects the progression of cooling and crystallization. The fraction of enriched end-member, X_e, present in each of the whole-rock samples can be calculated in the same way as described for the melt inclusions above (Fig. 8c). To aid comparison of the whole-rock data with those of the melt inclusions in Figs 6 and 7, the whole-rock X_e are plotted against the composition of the olivine expected to be in equilibrium with the whole-rock. The X_e are most variable in whole-rock compositions in equilibrium with olivines with a forsterite content of ~87 mol %. When the mixing parameter, *M*, is calculated for the Theistareykir and Krafla whole-rock compositions, there is a drop in *M* with decreasing forsterite content above Fo_{87} and then a rise in *M* between Fo_{87} and Fo_{75}. This pattern is qualitatively similar to that observed for the melt inclusions in Fig. 7 and may also be accounted for by the establishment of variation by supply of mantle melts followed by coupled mixing and crystallization. However, the total range of whole-rock compositions is smaller than that of the melt inclusions, so the minimum value of *M* observed for the whole-rock is 0·92.

Although the whole-rock data contain evidence for concurrent mixing and cooling of melts, these observations

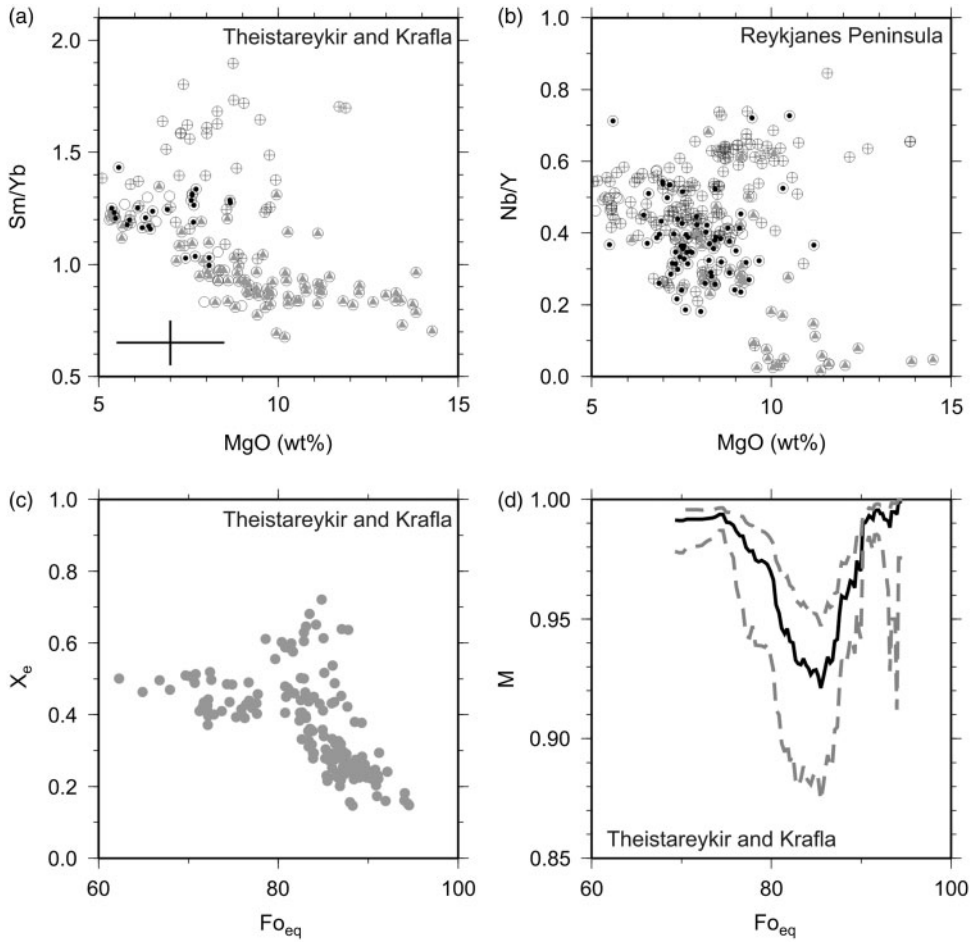

Fig. 8. Compositional variation within whole-rock samples from the Icelandic rift zones. (a) Samples from Theistareykir and Krafla. Circles containing crosses are glacial (>14 ka), circles containing grey triangles are early postglacial (7–14 ka) and and circles containing small black filled dots are <7 ka. The cross in the bottom left corner shows the typical range of variation found within a single eruption. Data from Nicholson *et al*. (1991) Nicholson & Latin (1992), Slater *et al*. (1998, 2001) and Maclennan *et al*. (2002). (b) Same as (a) but for Reykjanes Peninsula data of Gee *et al*. (1998*a*, 1998*b*). (c) Plot of the fraction of enriched end-member, X_e, for the whole-rock samples from Krafla and Theistareykir against the forsterite content of the olivine in Fe–Mg equilibrium with the whole-rock composition. The X_e is calculated in the same way as for the melt inclusions of Figs 4–6. The equilibrium olivine is calculated under the assumption that $K_d^{Fe-Mg} = 0{\cdot}3$ and that 90% of the Fe in the whole-rock is present as Fe^{2+}. (d) Variation in M against forsterite content of the olivine in equilibrium with the whole-rock samples from Krafla and Theistareykir. Line-markings the same as those in Figs 6 and 7.

record the mixing process in a different way to the melt inclusion compositions. It has already been demonstrated that the trace element variation within the whole-rock samples of individual eruptions is limited. The compositions of the single eruptions are controlled by mixing of diverse melts in a magma chamber, or set of magma chambers. Therefore, the variation in the whole-rock compositions from flow to flow reflects differences between the sets of magma chambers that feed single flows. The drop in the variation of X_e between flows with increasing evolution may reflect the increasing likelihood of physical juxtaposition and mixing with diverse melt batches with increasing residence time of melt in the crust (Fig. 9). A further point of interest is that the data in Fig. 8 show significantly different distributions of trace element compositions for glacial and early postglacial eruptions when the MgO content of the flow is >7 wt % MgO. This difference has been attributed to variation in mantle melting conditions related to glacial unloading (Maclennan *et al.*, 2002). However, more evolved rocks show relatively little variation in composition, and the trace element ratios of glacial and early postglacial rocks with <7 wt % MgO are similar. These observations indicate that mantle melts generated under different conditions and at different times are able to mix in the crust. The residence time of evolved melts in the crust that is implied by this observation may be a few thousand years or less, and is dependent upon temporal constraints on the rate of deglaciation and its translation into melt supply from the mantle.

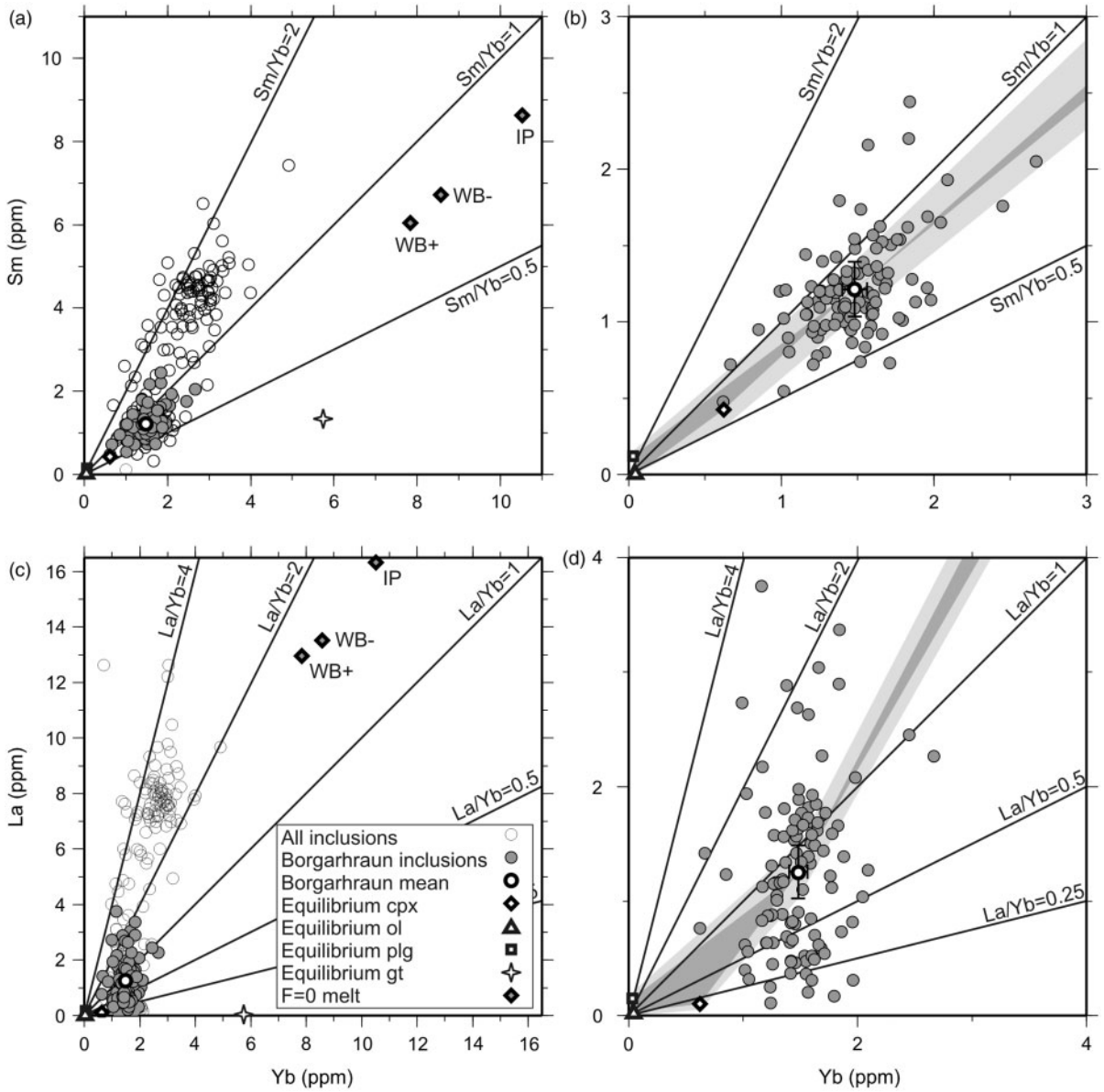

Fig. 9. Icelandic melt inclusion compositions. Plots (a) and (b) show Sm against Yb, and (c) and (d) show La against Yb. Plots (b) and (d) contain details of (a) and (c) close to the origin. A legend is provided in (c). In plots (a) and (c) the compositions of all of the Icelandic olivine-hosted melt inclusions used in this study are shown as open circles, apart from those from Borgarhraun, which are grey-filled circles. Only the Borgarhraun inclusions are shown in plots (b) and (d). The average Borgarhraun inclusion composition is marked as a white-filled circle with a thick outline and 1σ error bars plotted in (b) and (d). These error bars are based on the precision estimates for the Borgarhraun melt inclusion compositions from Maclennan *et al.* (2003*a*). The compositions of minerals in equilibrium with the Borgarhraun average were calculated using the partition coefficient parameterizations of Wood & Blundy (1997) for clinopyroxene, Bédard (2005) for olivine, Bédard (2006) for plagioclase and the experimental results of Hauri *et al.* (1994) for garnet. The compositions of small-degree mush-zone melts in equilibrium with a gabbro with the trace element composition of Borgarhraun (labelled 'F = 0 melt' on the legend) were calculated from these partition coefficients and the Borgarhraun average, assuming that the gabbro had a modal mineralogy of 50% plagioclase, 40% clinopyroxene and 10% olivine. This modal mineralogy is based on both the observed modal mineralogy of gabbroic nodules in Borgarhraun (Maclennan *et al.*, 2003*a*) and the major element trends of Theistareykir basalts (Maclennan *et al.*, 2001*a*). The point marked 'WB+' shows the melt composition calculated using the highest partition coefficients calculated for the Borgarhraun clinopyroxene from the method of Wood & Blundy (1997), that for 'WB–' is for the lowest partition coefficients, and the point marked 'IP' is based on the average composition of ion-probe measurements of Borgarhraun clinopyroxene from Maclennan *et al.* (2003*a*). The dark-grey shaded fields in (b) and (d) show the range of melt compositions that can be generated by reaction of the Borgarhraun average composition with cumulate minerals (trend to bottom left) or mixing with small-degree mush-zone melts (trend to top right). The lighter grey shaded fields show the range of melt compositions that can be generated if the Borgarhraun average estimated melt compositions are allowed to vary by the 1σ precision estimate of the ion probe analyses of the inclusions.

DISCUSSION

Rates of mixing and cooling

To compare the melt inclusion observations with the results of physical models of melt mixing, it is useful to convert the relative rates of mixing and change in host olivine composition, dM/dFo, into relative rates of mixing and cooling or crystallization. The dM/dFo for Borgarhraun and for melt inclusions from all 10 Icelandic eruptions that have been studied were calculated in a previous section from the results plotted in Figs 6 and 7. To convert variations in forsterite content into variations in melt temperature and extent of crystallization, it is necessary to use crystallization models based on parameterizations of experimental data. A range of melt compositions from the Theistareykir and Krafla dataset were modelled using the MELTS (Ghiorso & Sack, 1995), COMAGMAT (Ariskin *et al.*, 1993) and PETROLOG (Danyushevsky, 2001) fractional crystallization models. The model pressure of crystallization was varied from 0 to 1 GPa and the oxygen fugacity was fixed at one log unit beneath the fayalite–quartz–magnetite buffer. The models' results indicate that during the crystallization of gabbro, which takes place when the melt is in equilibrium with olivine less forsteritic than Fo_{89}, the relative rates of variation in fosterite content and cooling and crystallization are $2{\cdot}3^{\circ}C/mol\% < dT/dFo < 3{\cdot}5^{\circ}C/mol\%$ and $0{\cdot}04$ per mol $\% < df/f dFo < 0{\cdot}07$ per mol %, where df/fdFo is the fractional rate of change in extent of crystallization as a function of forsterite content. Therefore, given that the apparent rates of change of mixing and forsterite content over the gabbro crystallization interval are 0·02–0·03 per mol % it follows that the relative rate of mixing and cooling is $dM/dT = 0{\cdot}0094 \pm 0{\cdot}0036$ per °C and the rate of mixing and fractional change in extent of crystallization is $f dM/df = 0{\cdot}52 \pm 0{\cdot}23$.

In the analysis above it has been assumed that the crystallization of olivine is driven by temperature decreases rather than by magmatic degassing. This assumption is used because the volatile contents of Icelandic basalts and melt inclusions are low, with Gæsafjöll pillows containing 0·35 wt % H_2O and other rift zones eruptions from close to the studied flows containing <0·7 wt % H_2O (Nichols *et al.*, 2002). Extensive volatile degassing may not occur until depths of as little of 400 m for such Icelandic eruptions (Guilbaud *et al.*, 2007), much shallower than the lower crustal sites of crystallization of the olivines that host the melt inclusions of this study (Maclennan *et al.*, 2003*a*).

These relative rates of mixing and cooling can be used in future studies to constrain the fluid dynamical processes occurring within Icelandic magma chambers. The coupling of mixing and cooling can be achieved by convection, because convection not only enhances heat loss from the magma chamber but also stirs the melt and allows it to mix. Cooling rates of the melt in a laterally extensive sill should be proportional to the one-third power of the Rayleigh number in the chamber (Jaupart & Brandeis, 1986; Huppert, 2003). If the mixing rate in the sill is proportional to a different power of the Rayleigh number then the relative rates of mixing and cooling can be used to estimate the Rayleigh number and quantify the vigour of convection in magma chambers under Iceland. The viscosity of the magma will increase during cooling and crystallization, and this increase is likely to influence the mixing behaviour. However, more data are required to identify variation in the relative rates of mixing and cooling across the crystallization interval considered above.

Timescales

In addition to providing relative rates and mixing and cooling, some additional observations can be used to constrain absolute rates. Diffusion studies indicate that the re-equilibration of olivines and melt inclusions with their host melt is rapid. In a recent study, Spandler *et al.* (2007) inferred that a 50 μm melt inclusion at the centre of a 1 mm olivine will equilibrate with the host melt with an e-folding (63% re-equilibration) timescale of 40 years for Ce and 2 years for Lu. These calculations were performed assuming an equilibration temperature of 1300°C, similar to estimates of crystallization temperature for the Borgarhraun olivines (Maclennan *et al.*, 2001a, 2003*a*). It is expected that Ce will show similar behaviour to La, and Lu similar to that of Yb. The distribution of melt inclusion compositions in flows such as Borgarhraun and their relationship to the host lava compositions indicate, however, that diffusive re-equilibration of trapped inclusions has not occurred. The maximum spread in melt inclusion compositions is found in olivines containing between 87 and 90 mol % forsterite. However, the average composition of these inclusions is the same as that of the host flow. The preservation of the large range in inclusion compositions indicates that the similarity of the melt inclusion and whole-rock mean is dictated by mixing of melts rather than by diffusive equilibration of trapped inclusions. Further evidence for incomplete equilibration is provided by the variation in trace element concentrations and ratios noted within single olivine crystals (Slater *et al.*, 2001). Given that typical melt inclusions in primitive flows such as Borgarhraun have a diameter of 100 μm and occur in olivines of 5 mm diameter, the characteristic timescale of equilibration for La is expected to be close to 600 years (Qin *et al.*, 1992).

The Fe–Mg disequilibrium between olivines and their host lavas is demonstrated in Fig. 3. This disequilibrium can be used to estimate the time that the olivine has been in contact with the mixed carrier melt. To maintain disequilibrium in a 5 mm diameter olivine, such as the largest from Stapafell, indicates residence times of less than 3000 years if the diffusion rates of forsteritic olivine at 1200°C

of Chakraborty (1997) are used, or less than 1000 years at 1300°C. Compositional profiles across crystal edges and the margins of melt inclusions from Borgarhraun and Stapafell show that the Fe–Mg diffusion lengths are of the order of 50 μm or less, implying residence times of 10 years or less (Danyshevsky *et al.*, 2002; Costa & Dungan, 2005). Both the trace element and Fe–Mg data therefore indicate that the residence time of the olivines in the evolved, mixed carrier melt is short. Although the Fe–Mg zonation possibly records only the final entrainment of olivine into a slightly more evolved melt composition, the trace element variation data indicate that the timescales of mixing are less than a few hundred years.

Further evidence for limited residence time of melt in the Icelandic crust comes from the lag time of 1 kyr or less between deglaciation and increased eruption rates (Maclennan *et al.*, 2002). Furthermore, study of the U-series disequilibrium and degree of evolution of recent eruptions from the Vestmann islands indicates that extensive evolution can occur within 20 years in Icelandic magma chambers (Sigmarsson, 1996). The timescales of the concurrent mixing and cooling inferred from the data in Figs 6 and 7 are years to hundreds of years. The results of the crystallization models described in the previous section indicate that the cooling interval associated with the range of olivine compositions displayed in Fig. 7 is ~200°C. The rates of cooling in Icelandic magma chambers are therefore likely to be between 0·2 and 20°C/year. These observations may also be used to constrain the fluid dynamics of Icelandic magma chambers.

Disentangling mantle and crustal origins of trace element variation

Suites of Icelandic basalt samples show strong correlations between incompatible trace element ratios and isotopic composition. These correlations are found both on the scale of individual volcanic systems (Zindler *et al.*, 1979; Stracke *et al.*, 2003; Thirlwall *et al.*, 2004) and across the island as a whole (Hémond *et al.*, 1993; Kokfelt *et al.*, 2006). The relationships between the trace element and isotopic composition of these samples strongly indicate that mantle melts with variable compositions are fed to individual volcanic systems over timescales of 1 kyr or less (Maclennan *et al.*, 2002; Maclennan, 2008). It is also widely accepted that REE variation in Icelandic olivine-hosted melt inclusions reflects variation in the composition of mantle melts (Gurenko & Chaussidon, 1995; Slater *et al.*, 2001; Maclennan *et al.*, 2003*a*, 2003*b*; Maclennan, 2008).

Nevertheless, a number of researchers have highlighted the ability of magma chamber processes to generate variation in incompatible trace element ratios within the oceanic crust. Trace element depleted melts may be generated by reaction of primary melts with the cumulate minerals in the lower oceanic crust (Bédard, 1993). Trace element enriched melts with primitive major element compositions may be generated by addition of interstitial melts from the cumulate pile to a convecting magma body (Langmuir, 1989; Meurer & Boudreau, 1998). Recently, the composition of olivine-hosted melt inclusions from mid-ocean ridge basalt (MORB) has been reinterpreted in terms of such processes, with extreme trace element depletion in melt inclusions being generated by reaction of cumulate plagioclase and/or clinopyroxene with more enriched carrier melt and the host olivine (Danyushevsky *et al.*, 2004). This process is referred to as dissolution–reaction–mixing (DRM). If DRM is important, then substantial local trace element variability can be introduced to a homogeneous parental melt, and the melt inclusion compositions need not correspond to the compositions of significant volumes of melt. Accordingly, Danyushevsky *et al.* (2004) have urged caution in the interpretation of melt inclusion compositions in terms of mantle melt variability.

Sr anomalies generated by crustal processes

The influence of reaction between cumulates and percolating primitive melts on trace element systematics has recently been evaluated by Gurenko & Sobolev (2006), who found that positive Sr anomalies in basaltic glasses from the Miðfell eruption in SW Iceland could be accounted for by chromatographic effects during flow and reaction between basalts and gabbroic cumulates. Approximately 5% of the melt inclusions used in the present study (12 out of 203) have pronounced positive Sr anomalies, with $Sr/Sr^* > 2$. This quantity was defined following Gurenko & Sobolev (2006) as $Sr/Sr^* = Sr_n/(Ce_n \times Nd_n)^{0.5}$ with the n subscript applied to chondrite-normalized values. Such anomalies are independent of the Pb isotopic composition of the inclusions (Maclennan, 2008) and the correlation between Sr/Sr^* and trace element ratios such as La/Yb is weak, with $r = -0.17$ for Borgarhraun inclusions. The full range of La/Yb (0·09–3·23) is present in Borgarhraun inclusions that do not possess significant Sr anomalies ($Sr/Sr^* < 1$). These observations indicate that the Sr anomalies are produced by crustal processes. However, further considerations, outlined below, strongly indicate that much of the trace element variation found within melt inclusions from single flows originates from variability in the composition of mantle melts fed into the roots of single eruptions.

Pb isotope evidence for mantle origin of inclusion variability

Olivine-hosted melt inclusions from the Háleyjabunga picrite of the Reykjanes Peninsula in SW Iceland show a strong correlation between their trace element and isotopic composition, with trace element ratios such as Nb/Y and $^{208}Pb/^{206}Pb$ both displaying a significant range of values and lying within error of binary mixing trends between enriched and depleted melt inclusion compositions (Maclennan, 2008). Furthermore, the compositions of inclusions from Háleyjabunga and neighbouring Stapafell

form an array of trace element and lead isotope ratios that are coincident with whole-rock data from the Reykjanes Peninsula (Thirlwall *et al.*, 2004; Maclennan, 2008). The isotopic variation observed in these samples cannot be generated in the young Icelandic crust, and must reflect heterogeneity in the composition of the mantle under the active volcanic zones (Zindler *et al.*, 1979; Hémond *et al.*, 1993; Thirlwall *et al.*, 2004; Maclennan, 2008). The relationship between the isotopic and incompatible trace element composition of the Reykjanes melt inclusions therefore indicates that the incompatible trace element variation in olivine-hosted melt inclusions originates in the mantle. The DRM and *in situ* crystallization processes favoured by Danyushevsky *et al.* (2004) can generate neither the observed isotopic variation in the inclusions nor the relationship between the incompatible trace element composition and isotopic composition of the inclusions. Indeed, DRM processes should create significant scatter in the melt inclusion trace element ratio at a fixed isotopic composition, and would offset melt inclusion compositions from the compositional arrays observed in whole-rock lava compositions.

REE element evidence for a mantle origin of inclusion variability

The trace element systematics also indicate that mantle processes are responsible for part of the variation in incompatible element composition of the melt inclusions. The ability of crustal processes to fractionate trace elements is dependent on the partition coefficients of the phases present within the Icelandic crust. Numerous studies of Icelandic xenoliths and their host basalts have found that the dominant phases in cumulate materials in equilibrium with primitive rift-zone basalts and picrites are olivine, clinopyroxene and plagioclase, with chromian spinel as an accessory phase (Maclennan *et al.*, 2003*a*; Gurenko & Sobolev, 2006; Holness *et al.*, 2007; and references within). The partition coefficients of these phases can be estimated using parameterizations that link the partition coefficient to the major element composition of the crystal or host melt, such as those of Wood & Blundy (1997) for clinopyroxene, Bédard (2005) for olivine, and Bédard (2006) or Bindeman *et al.* (1998) for plagioclase. Alternatively, the trace element composition of phases likely to be involved in crustal processes can be determined by direct measurement (Maclennan *et al.*, 2003*a*; Danyushevsky *et al.*, 2004). A distinctive feature of Icelandic melt inclusions is that large variation in the concentration of incompatible elements such as La or Nb is present in inclusions that have a relatively limited range of content of less incompatible elements such as Yb or Y (Fig. 9). For instance, Borgarhraun inclusions display a factor of 35 variation in La, but only a factor of four variation in Yb.

The relatively low partition coefficient of Yb in clinopyroxene, plagioclase and olivine causes DRM to reduce the La content of the melt with a similar relative drop in Yb. Therefore, simple DRM processes cannot generate a large range in La or Sm with a limited shift in Yb. This problem was noted by Danyushevsky *et al.* (2004), who, in their modelling of a depleted inclusion, S1-OL24-GL3, from the Siqueiros Transform Fault, found an acceptable fit to the La and Sr contents of the inclusion, but provided a calculated Y concentration that was a factor of 3·7 times lower than that of the observed inclusion. They were not able to offer any explanation for this misfit. For the DRM modelling, a uniform initial carrier melt composition is required, and in Fig. 9 the average Borgarhraun melt inclusion composition is used as an estimate of this carrier. It makes no difference to the arguments presented below if the average Borgarhraun whole-rock composition is used instead of the average melt inclusion composition. The partitioning of La, Sm and Yb into olivine, plagioclase and chromian spinel is negligible. Therefore, the ability of DRM to alter La/Yb and Sm/Yb ratios, equivalent to reducing La or Sm with little or no drop in Yb, is controlled by the clinopyroxene partitioning. The trace element partition coefficients were estimated from the major element composition of Borgarhraun clinopyroxenes (Maclennan *et al.*, 2003*a*) using the method of Wood & Blundy (1997). The REE composition of the clinopyroxene in equilibrium with the average Borgarhraun melt composition was calculated using these partition coefficients. The composition of clinopyroxene in equilibrium with the mean Borgarhraun melt can also be estimated from the microprobe measurements of Borgarhraun clinopyroxene compositions by Maclennan *et al.* (2003*a*). The clinopyroxene compositions calculated from the partition coefficients are ~25% higher than the average observed clinopyroxene for the middle REE (REE) and HREE, and 50% higher for LREE. The arguments presented below hold true if either the predicted equilibrium clinopyroxene or the observed clinopyroxene compositions are used in the DRM calculation.

The composition of the average Borgarhraun melt and the crystalline phases in equilibrium with this melt are shown in Fig. 9. The range of melt compositions that can be generated by reaction between the carrier melt and olivine, clinopyroxene and plagioclase are shown as grey shaded regions to the bottom left of the carrier melt compositions in Fig. 9b and d. This DRM mechanism cannot reproduce the composition of melt inclusions with low La and low Sm but Yb similar to that of the carrier melt. These inclusions lie below the grey shaded bands in Fig. 9b and d.

The DRM processes described by Danyushevsky *et al.* (2004) can only produce inclusions more depleted than the carrier melt. Those workers therefore suggested that trace element enriched inclusions were generated by interaction of the carrier melt with evolved residual mush-zone melts. The composition of such residual melts is controlled

by the partition coefficients of the cumulus phases. In crustal cumulate xenoliths from Borgarhraun, olivine, clinopyroxene and plagioclase are the cumulus phases (Maclennan *et al.*, 2003*a*). The partition coefficients calculated above were used to estimate the composition of small-degree melts in equilibrium with a gabbro with the trace element composition of the average Borgarhraun melt. The small-degree melts have predicted La/Yb and Sm/Yb that are significantly lower than those observed in the most enriched melt inclusions (Fig. 9a and c). Many of the enriched inclusions lie above the grey field that indicates the locus of melts that can be produced by mixing the Borgarhraun average melt with the predicted small-degree mush-zone melt (Fig. 9b and d). These calculations demonstrate that the large variations in La and Sm with limited variation in Yb observed in the Borgarhraun melt inclusions are difficult to reproduce by processes involving the phases known to exist in Borgarhraun cumulates. The composition of garnet in equilibrium with the Borgarhraun average melt is shown in Fig. 9a and c. HREE are compatible in garnet, and melting in the presence of garnet-bearing lithologies can generate large variations in La and Sm with only modest variations in Yb. It is therefore likely that part of the trace element variation preserved in the Borgarhraun melt inclusions arises during mantle melting. This conclusion is strongly supported not only by the relationship between isotopic and trace element variation in the melt inclusions, but also by the trace element systematics alone.

Location of mixing

Crystallization of Icelandic basalts occurs over a range of depths in the crust and, possibly, uppermost mantle. Estimates of the depth of crystallization under Krafla and Theistareykir have been provided by application of barometers based on clinopyroxene–melt equilibrium, melt saturation with olivine–clinopyroxene–plagioclase and the crystallization order (Maclennan *et al.*, 2001*l*, 2003*a*, 2003*b*). All three of the barometric methods indicate that crystallization of primitive basalts occurs at pressures of 0·7–1·0 GPa, close the base of the crust at 20–30 km. More evolved basalts, containing <9 wt % MgO, typically show crystallization pressures close to 0·5 GPa, corresponding to shallower, mid-crustal, depths. The improved clinopyroxene–melt barometer of Putirka *et al.* (2003) was reapplied to the Krafla and Theistareykir dataset. Clinopyroxenes with Mg-numbers of 85–90 record equilibration pressures of 0·7–1·0 GPa, whereas those with Mg-numbers of 75–80 give pressures of 0·4–0·7 GPa. These results reconfirm the presence of a large range of crystallization depths under the neovolcanic zones of Iceland. Additionally, the results indicate that melts deeper in the crust have crystallized less and mixed less than melts in the mid-crust. Melts in magma chambers close to the Moho may retain compositional variation reflecting variation derived from mantle processes. However, extensive mixing in lower crustal magma chambers destroys this variation. Magma batches that ascend to mid-crustal magma chambers preserve little of the initial variation present in the near-Moho chambers (Fig. 10).

The generation and destruction of compositional variability

The results of this study, when combined with the Pb isotope results of Maclennan (2008), can be used to construct a model of the generation and destruction of trace element variability under Iceland. The trace element composition of melts generated in the mantle is variable for two reasons. First, the Pb isotope data show that the composition of the mantle source entering the melting region is variable. Second, the fractional melting process generates substantial trace element variation. These variable melt compositions are transported towards the surface in high-porosity channels. Mixing may occur in the channels and the results of the models of Spiegelman & Kelemen (2003) indicate that melts travelling in the centre of channels at a given depth are mixtures of melts produced at deeper levels. However, the channel margins transport melts that are generated locally, in the low-porosity regions between the channels. One consequence of these models of channel flow is that the composition of melt supplied from the mantle to the crust may show a bimodal distribution, with channel centres transporting melts slightly more enriched that the mean composition and channel margins containing extremely depleted melts (Fig. 10). Subsequent mixing between these two end-member melt compositions in magma chambers can generate the binary mixing relationships observed in the Pb isotope and trace element systematics (Maclennan, 2008).

The record of mixing in magma chambers is provided by the relationship between the variation in melt inclusion compositions and that of their host olivines. Some mixing may occur in magma chambers prior to the onset of crystallization and the importance of this mixing stage is therefore poorly constrained. Mixing is coupled to cooling and crystallization. A possible cause of concurrent mixing and cooling is convection in magma chambers. Convective motions not only enhance heat loss from the magma chamber but also result in stirring of compositionally heterogeneous melts. Accordingly, variation in any trace element concentration or ratio that is not strongly influenced by crystallization is diminished by mixing. The observations therefore indicate that magma chamber processes act to destroy variation in trace element ratios such as Sm/Yb or Nb/Y. These processes occur in magma bodies at a range of depths in the Icelandic crust and uppermost mantle, with crystallization commencing at depths close to the Moho. Magma is occasionally supplied directly from deep magma chambers to the surface, to produce eruptions such as Borgarhraun.

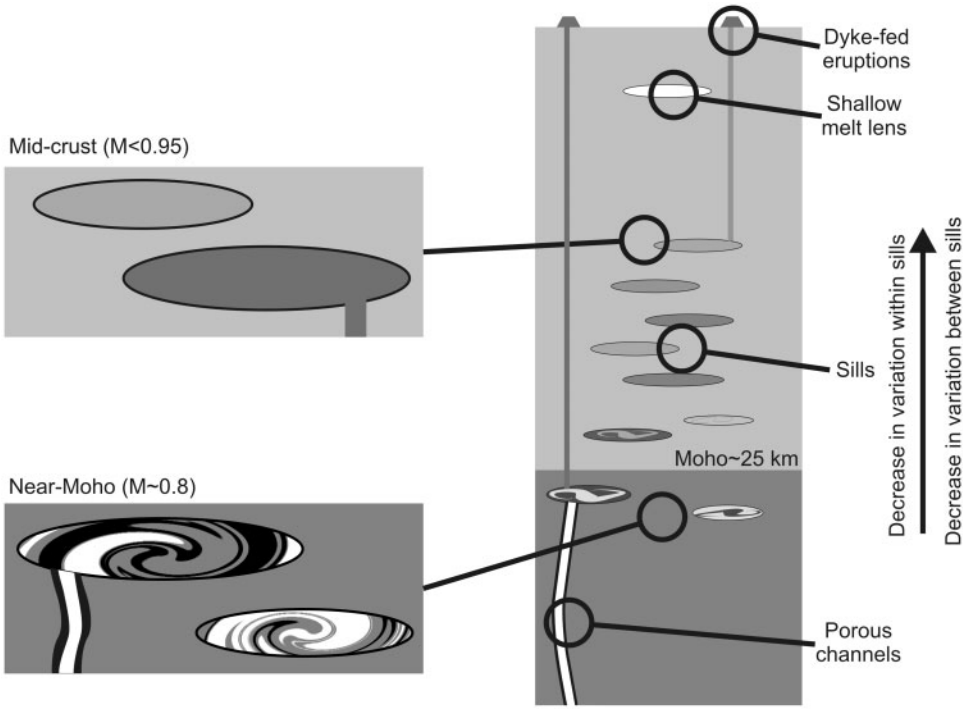

Fig. 10. Schematic synthesis of melt mixing under Iceland. Melt pictured in channels or sills is shaded according to its X_e, with dark shading showing more depleted melts with lower X_e. The vertical channels in the mantle transport variable melt compositions are as envisaged by Spiegelman & Kelemen (2003). These melts are fed to magma bodies in the uppermost mantle and lower crust where crystallization and mixing occurs. These bodies are shown as sills in this schematic illustration. Sometimes dykes can supply magma directly from the deep sills to the surface for eruptions. If, however, melt ponds in shallower magma chambers then mixing and crystallization will further proceed. The sizes and spacings of the melt channels and sills are not well constrained. Further details are given in the main text.

Magma may also pond at shallow levels within the crust, where mixing and crystallization continue. Compositional quantities that reflect variation in the composition of mantle melts supplied to the system have been effectively homogenized before they leave mid-crustal magma chambers. Magma chambers processes such as *in situ* crystallization (Langmuir, 1989), replenishment–tapping–fractionation (O'Hara, 1977) and assimilation–fractional crystallization (DePaolo, 1981) may produce variation in trace element ratios. However, over the crystallization interval considered in Figs 6–8 the importance of such processes is secondary in comparison with homogenization by melt mixing. In contrast, evolved basalts, andesites and rhyolites of the Krafla system, which contain <5 wt % MgO, have incompatible trace element, oxygen and thorium isotopic compositions consistent with the domination of AFC as the agent of magmatic evolution (Nicholson *et al.*, 1991). These processes are thought to operate in the shallow crust under Krafla (Jónasson, 2007). The transition from concurrent mixing and crystallization in the lower and mid-crust to AFC in the upper crust may reflect the sluggish mixing of high-viscosity evolved melts. Alternatively, assimilation of crustal melts may be facilitated in the shallow crust, where hydrothermal alteration is most intense (Jónasson, 2007).

CONCLUSIONS

For each of the 10 studied eruptions in the neovolcanic zones of Iceland, the trace element compositions of olivine-hosted melt inclusions are more variable than those of whole-rock samples of the carrier lava. The average composition of the melt inclusions is similar to that of the average of the host lava whole-rock samples. In Borgarhraun, the average La/Yb of melt inclusions remains almost constant in olivines containing less than 90 mol % forsterite. Both the average and distribution of melt inclusion compositions differ significantly between closely spaced eruptions. These observations indicate that the olivines found in lava flows from the neovolcanic zones of Iceland are not xenocrysts and are genetically related to the magma that carries them to the surface. Melts with compositions similar to those of the melt inclusions crystallize and mix to generate the carrier magma.

The trace element compositional variation of melt inclusions is related to the composition of the olivine host. The Borgarhraun eruption shows a significant decrease in variation of the La/Yb of melt inclusions as the fosterite content of the host olivine drops from 90 to 86 mol %. A similar decrease in variation is recorded in a compilation of all available melt inclusions ($N = 243$) in 10 eruptions

from the neovolcanic zones of Iceland. The deviation between the melt inclusion composition and the flow average decreases as the forsterite content of the host olivine drops from 90 to 76 mol %. Mixing and crystallization are therefore concurrent in magma chambers under Iceland. These processes occur in chambers at a range of depths in the crust and uppermost mantle. Primitive melts crystallize near the Moho at 20–30 km depth, and the extent of crystallization and mixing appears to increase with decreasing depth in the crust.

Mixing and cooling can be coupled by convective motions in magma chambers. These motions both stir melts with different trace element compositions and lead to increased heat fluxes from magma chambers. Melt inclusion and olivine compositions can be used to quantify relative rates of mixing and cooling in lower crustal magma chambers. The rate of change of the mixing parameter, M, with respect to estimated melt temperature is $dM/dT = 0{\cdot}0094 \pm 0{\cdot}0036$ per °C. It is hoped that this rate can be used to constrain the fluid dynamical properties of basaltic magma chambers.

ACKNOWLEDGEMENTS

The Natural Environment Research Council is thanked for the provision of a postdoctoral fellowship (NER/I/S/2002/00609/2) to the author. Access to the Natural Environment Research Council Ion Microprobe Facility hosted at the University of Edinburgh is also greatly appreciated, and the staff of the Facility are thanked for their dedicated assistance during the data acquisition. Pete Hill, Anthony Newton and David Steele helped with the electron microprobe analyses of the inclusions and their olivine hosts. Godfrey Fitton, Nic Odling, Rob Ellam and Valerie Olive were instrumental in the acquisition of the whole-rock data. The arguments contained within this paper were refined, clarified and strengthened by thoughtful, constructive and challenging reviews by Jon Davidson, John Sinton and Leonid Danyushevsky. The editorial handling of the paper by Marjorie Wilson is also much appreciated.

SUPPLEMENTARY DATA

Supplementary data for this paper are available at *Journal of Petrology* online.

REFERENCES

Ariskin, A. A., Barmina, G. S., Frenkel, M. Ya. & Nielsen, R. L. (1993). COMAGMAT: a Fortran program to model magma differentiation processes. *Computers and Geosciences* **19**, 1155–1170.

Bédard, J. H. (1993). Oceanic crust as a reactive filter: Synkinematic intrusion, hybridization, and assimilation in an ophiolitic magma chamber, western Newfoundland. *Geology* **21**, 77–80.

Bédard, J. H. (2005). Partitioning coefficients between olivine and silicate melts. *Lithos* **83**, 394–419.

Bédard, J. H. (2006). Trace element partitioning in plagioclase feldspar. *Geochimica et Cosmochimica Acta* **70**, 3717–3742.

Bindeman, I. N., Davis, A. M. & Drake, M. J. (1998). Ion microprobe study of plagioclase–basalt partition experiments at natural concentration levels of trace elements. *Geochimica et Cosmochimica Acta* **62**, 1175–1193.

Chakraborty, S. (1997). Rates and mechanisms of Fe–Mg interdiffusion in olivine at 980°–1300°C. *Journal of Geophysical Research* **102**, 12317–12331.

Costa, F. & Dungan, M. (2005). Short time scales of magmatic assimilation from diffusion modeling of multiple elements in olivine. *Geology* **33**, 837–840.

Danckwerts, P. V. (1953). Theory of mixtures and mixing. *Research (London)* **6**, 355–361.

Danyushevsky, L. V. (2001). The effect of small amounts of H_2O crystallisation of mid-ocean ridge and backarc basin magmas. *Journal of Volcanology and Geothermal Research* **110**, 265–280.

Danyushevsky, L. V., Sokolov, S. & Falloon, T. J. (2002). Melt inclusions in olivine phenocrysts: using diffusive re-equilibration to determine the cooling history of a crystal, with implications for the origin of olivine-phyric volcanic rocks. *Journal of Petrology* **43**, 1651–1671.

Danyushevsky, L. V., Leslie, R. A. J., Crawford, A. J. & Durance, P. (2004). Melt inclusions in primitive olivine phenocrysts: The role of localized reaction processes in the origin of anomalous compositions. *Journal of Petrology* **45**, 2531–2553.

Davidson, J. P., Morgan, D. J., Charlier, B. L. A., Harlou, R. & Hora, J. M. (2007). Microsampling and isotopic analysis of igneous rocks: implications for the study of magmatic systems. *Annual Review of Earth and Planetary Sciences* **35**, 273–311.

DePaolo, D. J. (1981). Trace element and isotopic effects of combined wallrock assimilation and fractional crystallization. *Earth and Planetary Science Letters* **53**, 189–202.

Einarsson, P. & Sæmundsson, K. (1987). Earthquake epicenters 1982–1985 and volcanic systems in Iceland (map). In: Sigfússon, Th. (ed.) *Í Hlutarsins Eðli: Festschrift for Thorbjorn Sigurgeirsson.*. Reykjavík: Menningarsjóður.

Fitton, J. G., Saunders, A. D., Larsen, L. M., Hardarson, B. S. & Norry, M. J. (1998). Volcanic rocks from the southeast Greenland margin at 63°N: Composition, petrogenesis and mantle sources. In: Saunders, A. D., Larsen, L. C. & Wise, S. W., Jr (eds) *Proceedings of the Ocean Drilling Program, Scientific Results, 152.* College Station, TX: Ocean Drilling Program, pp. 331–350.

Ford, C. E., Russell, D. G., Craven, J. A. & Fisk, M. R. (1983). Olivine–liquid equilibria—Temperature, pressure and composition dependence of the crystal–liquid cation partition coefficients for Mg, Fe^{2+}, Ca and Mn. *Journal of Petrology* **24**, 256–265.

Gee, M. A. M., Taylor, R. N., Thirlwall, M. F. & Murton, B. J. (1998*a*) Glacioisostacy controls chemical and isotopic characteristics of tholeiites from the Reykjanes peninsula, SW Iceland. *Earth and Planetary Science Letters*, **164**, 1–5.

Gee, M. A. M., Thirlwall, M. F., Taylor, R. N., Lowry, D. & Murton, B. J. (1998*b*) Crustal processes: Major controls on Reykjanes Peninsula lava chemistry, SW Iceland. *Journal of Petrology*, **39**, 819–839.

Ghiorso, M. S. & Sack, R. O. (1995). Chemical mass transfer in magmatic processes. 4. A revised and internally consistent thermodynamic model for the interpolation and extrapolation of liquid–solid equilibria in magmatic systems at elevated temperatures and pressures. *Contributions to Mineralogy and Petrology* **119**, 197–212.

Guilbaud, M.-N., Blake, S., Thordarson, T. & Self, S. (2007). Role of syn-eruptive cooling and degassing on textures of lavas from the

AD 1783–1784 Laki Eruption, South Iceland. *Journal of Petrology* **48**, 1265–1294.

Gurenko, A. A. & Chaussidon, M. (1995). Enriched and depleted primitive melts included in olivine from Icelandic tholeiites—origin by continuous melting of a single mantle column. *Geochimica et Cosmochimica Acta* **59**, 2905–2917.

Gurenko, A. A. & Sobolev, A. V. (2006). Crust–primitive magma interaction beneath neovolcanic rift zone of Iceland recorded in gabbro xenoliths from Miðfell, SW Iceland. *Contributions to Mineralogy and Petrology* **151**, 495–520.

Hauri, E. H., Wagner, T. P. & Grove, T. L. (1994). Experimental and natural partitioning of Th, U, Pb and other trace elements between garnet, clinopyroxene and basaltic melts. *Chemical Geology* **117**, 149–166.

Hémond, C., Arndt, N., Lichtenstein, U., Hofmann, A., Oskarsson, N. & Steinthorsson, S. (1993). The heterogeneous Iceland plume—Nd–Sr–O isotopes and trace element constraints. *Journal of Geophysical Research* **98**, 15833–15850.

Holness, M. B., Anderson, A. T., Martin, V. M., Maclennan, J., Passmore, E. & Schwindinger, K. (2007). Textures in partially solidified crystalline nodules: a window into the pore structure of slowly cooled mafic intrusions. *Journal of Petrology* **48**, 1243–1264.

Huppert, H. (2003). Geological fluid mechanics. In: Batchelor, G. K., Moffatt, H. K. & Worster, M. G. (eds) *Perspectives in Fluid Dynamics*. Cambridge: Cambridge University Press, pp. 447–506.

Jaupart, C. & Brandeis, G. (1986). The stagnant bottom layer of convecting magma chambers. *Earth and Planetary Science Letters* **80**, 183–199.

Jellinek, A. M. & Kerr, R. C. (1999). Mixing and compositional stratification produced by natural convection. Part 2. Applications to the differentiation of basaltic and silicic magma chambers and komatiite lava flows. *Journal of Geophysical Research* **104**, 7203–7219.

Jónasson, K. (2007). Silicic volcanism in Iceland: Composition and distribution within the active volcanic zones. *Journal of Geodynamics* **43**, 101–117.

Kelemen, P. B., Hirth, G., Shimizu, N., Spiegelman, M. & Dick, H. J. B. (1997). A review of melt migration processes in the asthenospheric mantle beneath oceanic spreading centers. *Philosophical Transactions of the Royal Society of London, Series A* **355**, 283–318.

Kilinc, A., Carmichael, I. S. E., Rivers, M. L. & Sack, R. O. (1983). The ferric–ferrous ratio of natural silicate liquids equilibrated in air. *Contributions to Mineralogy and Petrology* **83**, 136–140.

Kokfelt, T. F., Hoernle, K., Hauff, F., Fiebeg, J., Werner, R. & Garbe-Schonberg, D. (2006). Combined trace element and Pb–Nd–Sr–O isotope evidence for recycled oceanic crust (upper and lower) in the Iceland mantle plume. *Journal of Petrology* **47**, 1705–1749.

Langmuir, C. H. (1989). Geochemical consequences of *in situ* crystallization. *Nature* **340**, 199–205.

Maclennan, J. (2008). Lead isotope variability in olivine-hosted melt inclusions from Iceland. *Geochimica et Cosmochimica Acta* doi:10.1016/j.gca.2008.05.034.

Maclennan, J., McKenzie, D., Grönvold, K. & Slater, L. (2001*a*). Crustal accretion under northern Iceland. *Earth and Planetary Science Letters* **191**, 295–310.

Maclennan, J., McKenzie, D. & Grönvold, K. (2001*b*). Plume-driven upwelling under central Iceland. *Earth and Planetary Science Letters* **194**, 67–82.

Maclennan, J., Jull, M., McKenzie, D., Slater, L. & Grönvold, K. (2002). The link between volcanism and deglaciation in Iceland. *Geochemistry, Geophysics, Geosystems* **3**, paper number 1062.

Maclennan, J., McKenzie, D., Grönvold, K., Shimizu, N., Eiler, J. M. & Kitchen, N. (2003*a*). Melt mixing and crystallization under Theistareykir, northeast Iceland. *Geochemistry, Geophysics, Geosystems* **4**, paper number 8624.

Maclennan, J., McKenzie, D., Hilton, F., Grönvold, K. & Shimizu, N. (2003*b*). Geochemical variability in a single flow from northern Iceland. *Journal of Geophysical Research* **108**, paper number 2007.

Meurer, W. P. & Boudreau, A. E. (1998). Compaction of igneous cumulates part 1: Geochemical consequences for cumulates and liquid fractionation trends. *Journal of Geology* **106**, 281–292.

Nichols, A. R. L., Carroll, M. R. & Höskuldsson, Á. (2002). Is the Iceland hot spot also wet? Evidence from the water contents of undegassed submarine and subglacial pillow basalts. *Earth and Planetary Science Letters* **202**, 77–87.

Nicholson, H. & Latin, D. (1992). Olivine tholeiites from Krafla, Iceland—Evidence for variations in melt fraction within a plume. *Journal of Petrology* **33**, 1105–1124.

Nicholson, H., Condomines, M., Fitton, J. G., Fallick, A. E., Gronvold, K. & Rogers, G. (1991). Geochemical and isotopic evidence for crustal assimilation beneath Krafla, Iceland. *Journal of Petrology* **32**, 1005–1020.

O'Hara, M. J. (1977). Geochemical evolution during fractional crystallisation of a periodically refilled magma chamber. *Nature* **266**, 503–507.

Oldenburg, C. M., Spera, F. J., Yuen, D. A. & Sewell, G. (1989). Dynamic mixing in magma bodies: theory, simulations, and implications. *Journal of Geophysical Research* **94**, 9215–9236.

Olive, V., Ellam, R. M. & Wilson, L. (2001). A protocol for the determination of the rare earth elements at picomole level in rocks by ICP-MS: Results on geological reference materials USGS PCC-1 and DTS-1. *Geostandards Newsletter* **25**, 219–228.

Oskarsson, N., Helgason, O. & Steinthorsson, S. (1994). Oxidation state of iron in mantle-derived magmas of the Icelandic rift zone. *Hyperfine Interactions* **91**, 733–737.

Press, W. H., Teukolsky, S. A., Vetterling, W. T & Flannery, B. P. (1992). *Numerical Recipes*. Cambridge: Cambridge University Press.

Putirka, K. D. (2005). Mantle potential temperatures at Hawaii, Iceland, and the mid-ocean ridge system, as inferred from olivine phenocrysts: Evidence for thermally driven mantle plumes. *Geochemistry, Geophysics, Geosystems* **6**, paper number Q05L08.

Putirka, K., Ryerson, F. J. & Mikaelian, H. (2003). New igneous thermobarometers for mafic and evolved lava compositions, based on clinopyroxene + liquid equilibria. *American Mineralogist* **88**, 1542–1554.

Qin, Z., Lu, F. & Anderson, A. (1992). Diffusive reequilibration of melt and fluid inclusions. *American Mineralogist* **77**, 565–576.

Saal, A., Hart, S., Shimizu, N., Hauri, E. & Layne, G. (1998). Pb isotopic variability in melt inclusions from oceanic island basalts, Polynesia. *Science* **282**, 1481–1484.

Sigmarsson, O. (1996). Short magma chamber residence time at an Icelandic volcano inferred from U-series disequilibria. *Nature* **382**, 440–442.

Sinton, J., Grönvold, K. & Saemundsson, K. (2005). Postglacial eruptive history of the Western Volcanic Zone, Iceland. *Geochemistry, Geophysics, Geosystems* **6**, paper number Q12009.

Slater, L., Jull, M., McKenzie, D. & Grönvold, K. (1998). Deglaciation effects on mantle melting under Iceland: results from the northern volcanic zone. *Earth and Planetary Science Letters* **164**, 151–164.

Slater, L., McKenzie, D., Grönvold, K. & Shimizu, N. (2001). Melt generation and movement beneath Theistareykir, NE Iceland. *Journal of Petrology* **42**, 321–354.

Sobolev, A. V. (1996). Melt inclusions in minerals as a source of principle petrological information. *Petrology* **4**, 209–220.

Sobolev, A. V. & Shimizu, N. (1993). Ultra-depleted primary melt included in an olivine from the Mid-Atlantic Ridge. *Nature* **363**, 151–154.

Spandler, C., O'Neill, H. S. & Kamenetsky, V. S. (2007). Survival times of anomalous melt inclusions from element diffusion in olivine and chromite. *Nature* **447**, 303–306.

Spiegelman, M. & Kelemen, P. B. (2003). Extreme chemical variability as a consequence of channelized melt transport. *Geochemistry, Geophysics, Geosystems* **4**, 1055, doi:10.1029/2002GC000336.

Stracke, A., Zindler, A., Salters, V. J. M., McKenzie, D., Blichert-Toft, J., Albarède, F. & Grönvold, K. (2003). Theistareykir revisited. *Geochemistry, Geophysics, Geosystems* **4**, 8507, doi:10.1029/2001GC000201.

Thirlwall, M. F., Gee, M. A. M., Taylor, R. N. & Murton, B. J. (2004). Mantle components in Iceland and adjacent ridges investigated using double-spike Pb isotope ratios. *Geochimica et Cosmochimica Acta* **68**, 361–386.

Wood, B. J. & Blundy, J. D. (1997). A predictive model for rare earth element partitioning between clinopyroxene and anhydrous silicate melt. *Contributions to Mineralogy and Petrology* **129**, 166–181.

Workman, R. K. & Hart, S. R. (2005). Major and trace element composition of the depleted MORB mantle (DMM). *Earth and Planetary Science Letters* **231**, 53–72.

Yaxley, G. M., Kamenetsky, V. S., Kamenetsky, M., Norman, M. D. & Francis, D. (2004). Origins of compositional heterogeneity in olivine-hosted melt inclusions from the Baffin Island picrites. *Contributions to Mineralogy and Petrology* **148**, 426–442.

Zindler, A., Hart, S. R., Frey, F. A. & Jakobsson, S. P. (1979). Nd and Sr isotope ratios and rare earth element abundances in Reykjanes Peninsula basalts—Evidence for mantle heterogeneity beneath Iceland. *Earth and Planetary Science Letters* **45**, 249–262.